JAWS: Predictive Inference Under Covariate Shift

Drew Prinster
Department of Computer Science
Johns Hopkins University
Baltimore, MD 21211
drew@cs.jhu.edu

Anqi Liu
Department of Computer Science
Johns Hopkins University
Baltimore, MD 21211
aliu@cs.jhu.edu

Suchi Saria
Department of Computer Science
Johns Hopkins University
Baltimore, MD 21211
ssaria@cs.jhu.edu

Abstract

We propose **JAWS**, a series of wrapper methods for distribution-free uncertainty quantification tasks under covariate shift, centered on our core method **JAW**, the **JA**ckknife+ **W**eighted with likelihood-ratio weights. JAWS also includes computationally efficient **A**pproximations of JAW using higher-order influence functions: **JAWA**. Theoretically, we show that JAW relaxes the jackknife+'s assumption of data exchangeability to achieve the same finite-sample coverage guarantee even under covariate shift. JAWA further approaches the JAW guarantee in the limit of either the sample size or the influence function order under mild assumptions. Moreover, we propose a general approach to repurposing any distribution-free uncertainty quantification method and its guarantees to the task of risk assessment: a task that generates the estimated probability that the true label lies within a user-specified interval. We then propose **JAW-R** and **JAWA-R** as the repurposed versions of proposed methods for **R**isk assessment. Practically, JAWS outperform the state-of-the-art predictive inference baselines in a variety of biased real world data sets for both interval-generation and risk-assessment auditing tasks.

1 Introduction

Auditing the uncertainty under data shift Principled quantification of predictive uncertainty is a key challenge in the development of machine learning for trustworthy AI, especially in high-stakes settings: appropriate uncertainty estimates enable users to calibrate how much they should or should not trust a given prediction [Thiebes et al., 2021, Ghosh et al., 2021, Tomsett et al., 2020, Bhatt et al., 2021]. Uncertainty-based predictor auditing can be thought of as a type of uncertainty quantification that is performed *post-hoc*, for example by a regulator without detailed knowledge of a predictor's architecture and with limited resources, but potentially with access to the trained model, unlabeled test data, and the data used for training [Schulam and Saria, 2019]. Data shift imposes significant challenges to uncertainty auditing tasks due to violation of the common machine learning assumption of the training and test data being distributed identically and independently (IID) [Ovadia et al., 2019, Ulmer et al., 2020, Zhou and Levine, 2021, Chan et al., 2020]. Therefore, it is essential to develop convenient tools for users or regulators to estimate predictive uncertainty for auditing tasks even when training data is biased.

Accepted in Thirty-ninth International Conference on Machine Learning (ICML 2022) Workshop on Distribution-Free Uncertainty Quantification.

Predictor auditing: interval generation In this work we distinguish between two types of uncertainty-based predictor auditing. We describe a first type of predictor auditing by the task of *interval generation*, which refers to a common goal in the distribution-free uncertainty quantification literature: to generate a predictive interval (or confidence interval) that covers the true label with at least some user-specified probability. For instance, an auditor may wish to generate confidence intervals around a prediction that contain the true label with at least, say 90% probability. Regardless of an auditor or user's choice of coverage probability, smaller interval widths correspond to higher confidence in the original prediction, whereas larger interval widths correspond to lower confidence in the original prediction.

Predictor auditing: risk assessment While predictive interval generation has been a central focus of the distribution-free uncertainty quantification literature, in some applications the converse computation may be more actionable: that is, estimation of the probability that a user-specified interval around a prediction contains the true label. We describe this type of predictor auditing task as *risk assessment* because a natural type of interval for a user to specify is one defined by an error threshold around a prediction, where the goal then becomes to estimate the probability that the true label is within the error threshold (or the "risk" that the label is outside the threshold). A concrete example of when such a risk-assessment audit may be more useful to a stakeholder than an interval-generation audit is the setting of chemical or radiation therapy dose prediction for cancer treatment, where administering the correct dosage within $5\% - 10\%$ is safety-critical. [1] Though the risk-assessment perspective to distribution-free uncertainty quantification has received less attention in the literature than the interval-generating perspective, as we will see, any interval-generating predictive inference method with a distribution-free coverage guarantee can be repurposed for the task of risk assessment with minor modifications.

Coverage and exchangability A *coverage guarantee* refers to a guaranteed lower bound to the probability that a given interval covers the true label for a test data point, and this guarantee provides the basis for both interval generation and risk assessment auditing. Standard conformal prediction methods [Vovk et al., 2005, Shafer and Vovk, 2008, Vovk, 2013] along with the jackknife+ [Barber et al., 2021], which we refer to together as "predictive inference" methods, provide a framework for generating predictive intervals with finite-sample guaranteed coverage, contingent on the assumption of data exchangeability (e.g., IID).

In common situations of dataset shift, however, the exchangeability assumption that underpins standard conformal prediction and the jackknife+ is violated. Empirically, standard conformal prediction methods suffer from worse coverage performance when dataset shift is present [Tibshirani et al., 2019, Podkopaev and Ramdas, 2021]. The jackknife+ method offers a compromise between the statistical drawback of standard split conformal prediction and the computational drawback of standard full conformal prediction [Barber et al., 2021]. Nonetheless, as with standard conformal prediction methods, the jackknife+ also suffers from worse empirical coverage performance in the presence of dataset shift. For example, as shown in the Figure 1, jackknife+ can suffer significant loss of coverage under covariate shift.

Covariate shift *Covariate shift* is a common type of dataset shift where the $Y|X$ distribution is the same between training and test data but the marginal X distributions are allowed to change [Sugiyama et al., 2007, Shimodaira, 2000]. Recent work has extended the conformal prediction framework to achieve coverage guarantees under covariate shift using a weighted version of conformal prediction with the weights given by likelihood ratios between the training and test distribution [Tibshirani et al., 2019]. However, weighted conformal prediction methods still suffer from the statistical drawback of sample splitting (in the case of weighted split conformal prediction) or from the computational

[1] Machine learning is being increasingly employed in cancer chemotherapy and radiotherapy for purposes including dose optimization [Feng et al., 2018, Huynh et al., 2020]. Dose errors are one of the most common types of errors in chemotherapy and radiotherapy, occurring when a patient is given a substantially higher or lower than optimal amount of chemical or radiation treatment [Weingart et al., 2018, Van Herk, 2004]. An overdose of either chemotherapeutics or radiation can be harmful or even lethal to a patient, whereas underdose can result in a reduced anticancer effect [Gurney, 2002]. A dose error is generally defined as a percentage deviation, between a prescribed dose and the dose that should have been prescribed, beyond some error tolerance: $5\% - 10\%$ is a commonly used deviation threshold for defining errors [Cohen et al., 1996, Van Herk, 2004]. Accordingly, the probability that the optimal dosage level lies within say 10% of the predicted dosage level may be of greater interest to a provider and their patient than identifying a predictive interval (which might extend beyond the predicted dosage $\pm 10\%$) with some predetermined coverage probability.

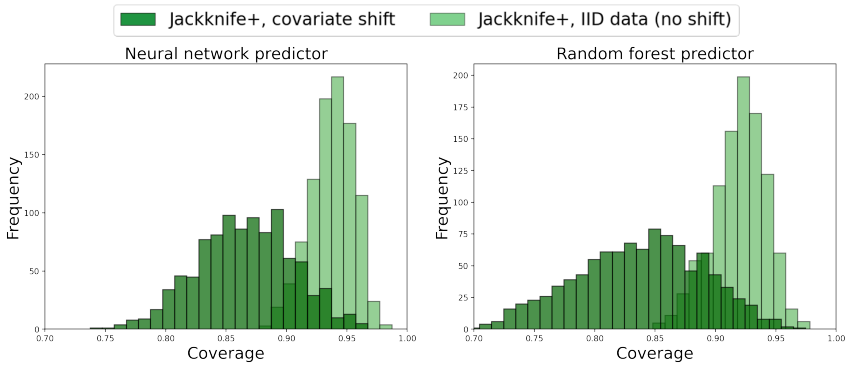

Figure 1: Jackknife+ loses coverage on the UCI airfoil dataset [Dua and Graff, 2017] due to covariate shift. Jackknife+ coverage on IID data is in light green and under covariate shift is in dark green, for a neural network (left) and a random forest predictor (right). The creation of the covariate shift is following the exponential tilting strategy. More details are in Sec. 5.

drawback of prohibitive retraining requirements (in the case of weighted full conformal prediction) [Tibshirani et al., 2019, Zeni et al., 2020, Ndiaye and Takeuchi, 2019]. Barber et al. [2022] recently proposed a weighted version of the jackknife+, but their theoretical and empirical results assume that the weights are fixed, rather than data-dependent like in our work (See Section 2.3 for more details).

Influence functions Influence functions (IFs) [Cook, 1977] have long been used in robust statistics to quantify how much a parameter estimate would change by removing or reweighting a datapoint from a sample, and in recent years the use of IFs in machine learning has become more widespread for uses such as improving model interpretability Koh and Liang [2017]. Recent work has leveraged IFs for approximating classic resampling uncertainty quantification methods including bootstrap [Schulam and Saria, 2019], jackknife, and leave-k-out cross validation [Giordano et al., 2019a] [Giordano et al., 2019b]. The intuition is that in each of these classic resampling approaches, any resampled set of the training data can be formulated as a reweighting of the data, and IFs can thereby approximate how the original model parameters would change if the model were to be retrained with the reweighted data. In the case of the jackknife+, influence functions can be used to approximate the parameters for the leave-one-out models without retraining the original model. The use of higher-order influence functions for approximating the jackknife+ was proposed by Alaa and Van Der Schaar [2020], but their work assumes exchangeable or IID train and test data.

In this work, we develop a predictor auditing method with a coverage guarantee under covariate shift. **Our contributions can summarized as follows**:

1. We develop JAW: a jackknife+ method weighted with likelihood-ratio weights for uncertainty quantification under covariate shift. To the best of our knowledge, this is the first in the literature. We provide a rigorous finite-sample coverage guarantee for JAW, the same coverage guarantee as the jackknife+ [Barber et al., 2021] while relaxing the data exchangeability assumption to allow for covariate shift.
2. We develop JAWA: a sequence of computationally efficient approximations to JAW that avoids retraining by leveraging higher-order influence functions. Under assumptions outlined in Giordano et al. [2019b] regarding the regularity of the data, Hessian of the objective (local strong convexity), and the existence of higher order derivatives, we provide an asymptotic guarantee for the coverage of the JAWA prediction interval in the limit of either the sample size or influence function order.
3. We propose a general approach to repurposing any interval-generating uncertainty quantification method for the task of risk assessment, with rigorous guarantees for the coverage probability estimation. Our approach applies to methods that assume exchangeable data and to methods like JAW and JAWA that allow for covariate shift—JAW-R and JAWA-R refer to the repurposed versions for risk assessment.
4. We demonstrate superior empirical performance of JAWS over other distribution-free predictive inference baselines on a variety of benchmark datasets under covariate shift.

Table 1 moreover provides a summary of the JAWs methods and a few of their key properties.

Table 1: Summary of key properties for JAWS methods.

Method	Task	Guarantee		Avoids retraining
		Finite sample	Asymptotic	
JAW	Interval generation	✓	✓	✗
JAWA	Interval generation	✗	✓	✓
JAW-R	Risk assessment	✓	✓	✗
JAWA-R	Risk assessment	✗	✓	✓

2 Preliminaries and Related Work

2.1 Covariate Shift

Under the covariate shift assumption, the $Y|X$ distribution is assumed to be the same between training and test data but the marginal X distributions are allowed to change:

$$\begin{aligned}(X_i, Y_i) &\overset{\text{iid}}{\sim} P = P_X \times P_{Y|X}, i = 1, ..., n \\ (X_{n+1}, Y_{n+1}) &\overset{\text{iid}}{\sim} \tilde{P} = \tilde{P}_X \times P_{Y|X}, \text{independently}\end{aligned} \tag{1}$$

This is a strong but common assumption for many dataset shift problems. Covariate shift is also closed related to data missingness and sample selection bias [Bickel et al., 2009]. Rich literature exist in this domain. The most prevalent method for correcting the shift is by applying likelihood ratio or "importance" weights [Sugiyama et al., 2007, Shimodaira, 2000]. Density ratio estimation is then a key subproblem of covariate shift correction [Sugiyama et al., 2012]. Other methods dealing with covariate shift include matching the (kernel) representation between the two distributions [Gretton et al., 2009, Yu and Szepesvári, 2012, Zhang et al., 2013, Zhao et al., 2021] and robust optimization [Liu and Ziebart, 2014, Chen et al., 2016, Duchi et al., 2019, Rezaei et al., 2021]. However, uncertainty quantification is relatively less explored under covariate shift. Recent work [Ovadia et al., 2019, Zhou and Levine, 2021, Chan et al., 2020] has emphasized the importance of a reliable uncertainty estimation under data shift, especially in the deep learning cases. Tibshirani et al. [2019] opens the possibility of conducting conformal prediction under covariate shift. We follow this line of work and focus on enabling the guaranteed predictive inference under covariate shift based on the jackknife+ method of Barber et al. [2021].

2.2 Standard conformal prediction

We assume a standard regression setup with training data $\{Z_1, ..., Z_n\} = \{(X_1, Y_1), ..., (X_n, Y_n)\}$ and a test point $Z_{n+1} = (X_{n+1}, Y_{n+1})$ where each X_i has dimension d, and a predictor $\widehat{\mu} = \mathcal{A}(\{(X_1, Y_1), ..., (X_n, Y_n)\})$, where $\mathcal{A}$ is the algorithm for fitting the model. Conformal prediction aims to generate a predictive interval or confidence interval (or region) $\widehat{C}^{\text{audit}}_{n,\alpha} : \mathbb{R}^d \to \{\text{subsets of } \mathbb{R}\}$ around the prediction $\widehat{\mu}(X_{n+1})$ that contains the true label Y_{n+1} with high probability: a small predictive interval corresponds to high confidence in the original prediction, while a large interval corresponds to low confidence. A central requirement for the predictive interval is the *coverage*: for a target coverage rate $1 - \alpha \in (0, 1)$, we would like the true label to reside in the confidence interval with high probability, that is for $\widehat{C}^{\text{audit}}_{n,\alpha}$ to satisfy

$$\mathbb{P}\Big\{Y_{n+1} \in \widehat{C}^{\text{audit}}_{n,\alpha}(X_{n+1}) \geq 1 - \alpha\Big\} \tag{2}$$

with flexible assumptions about the distribution of the training test data $(X_1, Y_1), ..., (X_{n+1}, Y_{n+1})$.

Since its initial development in the 1990s, the study of conformal prediction for producing predictive regions (in regression) or predictive sets (in classification) with guaranteed coverage has grown into a broader research field [Vovk et al., 2005, Shafer and Vovk, 2008, Vovk et al., 2009, Vovk, 2013, Burnaev and Vovk, 2014, Barber et al., 2022]. Traditional conformal prediction crucially relies on the notion of "exchangeability" of the data in two ways:

- The data $Z_i = (X_i, Y_i)$ are assumed to be exchangeable (for example, iid)
- The algorithm $\mathcal{A}$ that maps a data set to a fitte model $\widehat{\mu}$ must treat the data symmetrically

Given these assumptions, conformal prediction methods use a score function $\mathcal{S} : \mathbb{R}^d \times \mathbb{R} \to \mathbb{R}$ on the data, such as the residual score $\mathcal{S}(X_i, Y_i) = |Y_i - \widehat{\mu}(X_i)|$, to generate a distribution of "nonconformity" scores (or "conformity" scores) from which predictive regions can be derived. This kinds of estimates are also called *distribution-free* uncertainty estimates [Lei and Wasserman, 2014, Lei et al., 2018] to emphasize their applicability irrespective of distribution family, though this is not to be confused with independence from distribution *shift*. We consider the distribution-free uncertainty quantification under the covariate shift setting when the standard data exchangability condition is violated.

2.3 Weighted conformal prediction and beyond exchangeability

Tibshirani et al. [2019] develop the idea of *weighted exchangeability* for adapting conformal prediction to the covariate shift setting. Random variables $V_1, ..., V_n$ are called weighted exchangeable with weight functions $w_1, ..., w_n$ if their joint density f can be factorized as

$$f(v_1, ..., v_n) = \prod_{i=1}^{n} w_i(v_i) \cdot g(v_1, ..., v_n),$$

where g is independent of ordering on its inputs, that is, $g(v_{\sigma(1)}, ..., v_{\sigma(n)}) = g(v_1, ..., v_n)$ for any permutation σ of $1, ..., n$. In the case of covariate shift as in (1), Tibshirani et al. [2019] note that if the training distribution P_X and the test distribution $\tilde{P}_X$ are known, then the data $\{Z_i\}$ are weighted exchangeable with weights given by the likelihood ratio $w(X_i) = \mathrm{d}\tilde{P}_X(X_i)/\mathrm{d}P_X(X_i)$.

Note that in standard conformal prediction, if $\{V_i\}$ represent a set of nonconformity scores, then the empirical distribution of $\{V_i\}$ can equivalently be represented as a sum of uniform weighted point masses on the augmented real line, that is $\frac{1}{n+1}\sum_{i=1}^{n}\delta_{V_i} + \frac{1}{n+1}\delta_\infty$ (where δ_{V_i} denotes a point mass at V_i). Standard conformal predictive intervals are then generated from the quantiles of this uniform-weighted empirical distribution. By extension, weighted conformal prediction (for split or full conformal variants) generates confidence intervals from the *weighted* empirical distribution described as

$$\sum_{i=1}^{n} p_i^w(x)\delta_{V_i} + p_{n+1}^w(x)\delta_\infty$$

with weights defined as

$$p_i^w(x) = \frac{w(X_i)}{\sum_{j=1}^{n} w(X_j) + w(x)}, i = 1, ..., n, \qquad \text{and} \qquad p_{n+1}^w(x) = \frac{w(x)}{\sum_{j=1}^{n} w(X_j) + w(x)} \tag{3}$$

where the $p_i^w(x)$ can be thought of as normalized likelihood ratio weights (normalized with respect to the data $1, ..., n+1$).

Corollary 1 in [Tibshirani et al., 2019] provides the coverage guarantee of weighted conformal prediction: Assuming data from (1), that $\tilde{P}_X$ is absolutely continuous with respect to P_X, $w = \mathrm{d}\tilde{P}_X/\mathrm{d}P_X$, then for any score function $\mathcal{S}$, and any $\alpha \in (0, 1)$ and $x \in \mathbb{R}^d$, if

$$\widehat{C}_{n,\alpha}^w(x) = \Big\{ y \in \mathbb{R} : V_{n+1} \leq \text{Quantile}\Big(1 - \alpha; \sum_{i=1}^{n} p_i^w(x)\delta_{V_i} + p_{n+1}^w(x)\delta_\infty\Big)\Big\} \tag{4}$$

then $\widehat{C}_{n,\alpha}^w$ satisfies

$$\mathbb{P}\{Y_{n+1} \in \widehat{C}_{n,\alpha}^w(X_{n+1})\} \geq 1 - \alpha \tag{5}$$

However, weighted standard conformal prediction methods inherit the same statistical and computational issues as nonweighted standard conformal prediction. In particular, conformal prediction methods largely fall into two main groups, each with its own pitfall: split conformal and full conformal prediction [Vovk et al., 2005, Shafer and Vovk, 2008]. Split conformal prediction generates nonconformity scores on a labeled holdout dataset and is computationally efficient in that it does not require model retraining, but the requirement of having a holdout set can be impractical or lead to a drop in model accuracy if obtained from sample splitting Papadopoulos [2008], Lei et al. [2018], Vovk [2012]. On the other hand, full conformal prediction avoids sample splitting, but at the expense of a heavy computational cost due to the requirement of retraining the model on every possible target

value (or, in practice on a fine grid of target values) [Ndiaye and Takeuchi, 2019, Zeni et al., 2020]. Outside of standard conformal prediction, the recent jackknife+ [Barber et al., 2021] achieves a tradeoff between these statistical and computational considerations, which motivates our current work that extends the jackknife+ coverage guarantee to hold under covariate shift.

The recent work of [Barber et al., 2022] provides a novel extension of conformal prediction and the jackknife+ to unknown violations of the exchangeability assumption, and their "nonexchangeable jackknife+" is a weighted version of the jackknife+ that may initially appear similar to our proposed JAW method. However, the key difference is that Barber et al. [2022] assume that the weights are fixed and not data-dependent, and so their main results do not apply to data-dependent weightings of the jackknife+ like we propose in our current work. Though detailed comparison of the tradeoffs between fixed and data-dependent weightings is beyond the scope of our current study, it is worth noting that Barber et al. [2022] is able to compensate for unknown violations of exchangeability at the cost of a bounded but generally nonzero "coverage gap" (loss in coverage guarantee compared to if the data were exchangeable), whereas our JAW method assumes covariate shift but does not suffer from any similar coverage gap. [2] To the best of our knowledge, a weighted version of the jackknife+ with data-dependent, likelihood-ratio weights has not yet been investigated theoretically or empirically.

2.4 Jackknife+

The jackknife+ [Barber et al., 2021] is a recently developed alternative to split and full conformal prediction that offers a compromise between those methods' respective statistical and computational drawbacks at the cost of a slightly weaker coverage guarantee. It incorporates the leave-one-out methods for assessing the predictive accuracy like in cross validation [Butler and Rothman, 1980, Efron and Gong, 1983, Geisser, 1975, Stone, 1974] and is closely related to cross conformal prediction [Vovk et al., 2018]. The jackknife+ predictive interval can most easily be understood as a modification to a predictive interval based on the classic jackknife resampling method [Miller, 1974, Steinberger and Leeb, 2018, 2016] that it is inspired by.

Define the level $1-\alpha$ quantile on the empirical distribution of some values $v_1, ..., v_n$ as $\widehat{q}^{+}_{n,\alpha}\{v_i\}$, and define the level α quantile on the values as $\widehat{q}^{-}_{n,\alpha}\{v_i\}$. Then, letting $R_i^{LOO} = |Y_i - \widehat{\mu}_{-i}(X_i)|$ denote the leave-one-out residual for sample $Z_i = (X_i, Y_i)$, a predictive interval generated from classic jackknife resampling is defined as

$$\begin{aligned}\widehat{C}^{\text{jackknife}}_{n,\alpha}(X_{n+1}) &= \widehat{\mu}(X_{n+1}) \pm \widehat{q}^{+}_{n,\alpha}\{R_i^{LOO}\} \\ &= \Big[\widehat{q}^{-}_{n,\alpha}\{\widehat{\mu}(X_{n+1}) - R_i^{LOO}\}, \widehat{q}^{+}_{n,\alpha}\{\widehat{\mu}(X_{n+1}) + R_i^{LOO}\}\Big]. \end{aligned} \tag{6}$$

In contrast, the jackknife+ predictive interval as defined in [Barber et al., 2021] is obtained by replacing the full model prediction $\widehat{\mu}(X_{n+1})$ with $\widehat{\mu}_{-i}(X_{n+1})$ in (6), where $\widehat{\mu}_{-i} = \mathcal{A}\big((X_1, Y_1), ..., (X_{i-1}, Y_{i-1}), (X_{i+1}, Y_{i+1}), ..., (X_n, Y_n)\big)$, the model trained with the ith datapoint removed:

$$\widehat{C}^{\text{jackknife+}}_{n,\alpha}(X_{n+1}) = \Big[\widehat{q}^{-}_{n,\alpha}\{\widehat{\mu}_{-i}(X_{n+1}) - R_i^{LOO}\}, \widehat{q}^{+}_{n,\alpha}\{\widehat{\mu}_{-i}(X_{n+1}) + R_i^{LOO}\}\Big]. \tag{7}$$

[2] Additionally, it is important to take note of and contrast our work with an extension of the framework in Barber et al. [2022] to data-dependent weights that the authors briefly discuss in their Section 5.3, subsection titled "Fixed versus data-dependent weights" (though this extension is not a primary focus of their work). The authors do not propose a likelihood-ratio weighting of the jackknife+, but if one were to define the weights in Barber et al. [2022] for the jackknife+ as data-dependent, likelihood ratio weights like in our JAW method, then the extension discussed in Section 5.3 of Barber et al. [2022] would in general suffer from a nonzero coverage gap in their guarantee. In other words, the coverage guarantee for JAW that can be derived from the framework of Barber et al. [2022] is weaker than the guarantee we provide in our analysis. Specifically, under covariate shift assumptions and with $w_i = w(X_i)$ representing the likelihood ratio for datapoint i, the conditional total variation distance between the original ordered data $Z = (Z_1, ..., Z_{n+1})$ and the swapped data $Z^i = (Z_1, ..., Z_{i-1}, Z_{n+1}, Z_{i+1}, ..., Z_n)$ may be greater than zero, $\mathrm{d}_{TV}(Z, Z^i | w_1, ..., w_n, t_1, ..., t_{n+1}) > 0$. This is because under the covariate shift the training data $\{Z_1, ..., Z_n\}$ and test point Z_{n+1} are not exchangeable (they are weighted exchangeable, i.e., $wZ \overset{d}{=} w^i Z^i$), meaning that the unweighted data distributions Z and Z^i may have nonzero conditional total variation distance. In some severe covariate shift cases, it may even be the case that $\mathrm{d}_{TV}(Z, Z^i | w_1, ..., w_n, t_1, ..., t_{n+1}) \to 1$, which could result in a trivial coverage guarantee (e.g., only guaranteeing coverage ≥ 0).

[Barber et al., 2021] prove that, whereas no coverage guarantee is possible for the classic jackknife predictive interval (6), the jackknife+ prediction interval satisfies

$$\mathbb{P}\{Y_{n+1} \in \widehat{C}_{n,\alpha}^{\text{jackknife+}}(X_{n+1})\} \geq 1 - 2\alpha \tag{8}$$

with the same assumptions of exchangeable data and a symmetric algorithm as in standard conformal prediction. Accordingly, the coverage guarantee (8) for the jackknife+ does not hold under dataset shift such as covariate shift. In this paper, we apply importance weights from density ratios to jackknife+ and achieve the same coverage guarantee under covariate shift.

2.5 Higher-order influence function approximation of the jackknife+

For a weight vector variable $\omega \in \mathbb{R}^n$ and a fixed instance of the variable $\omega = \tilde{\omega}$ representing a specific reweighting of the data, let us denote $\widehat{\mu}_{\tilde{\omega}}$ as the refitted model and $\hat{\theta}(\tilde{\omega})$ as the refitted model parameters that would be obtained by retraining the model with data weights $\tilde{\omega}$. With our notation in this section we maintain some similarity to the notation in Giordano et al. [2019b] (whose method we implement in this work for computing influence functions), but we use the Greek character ω rather than w to disambiguate the IF data weights ω from the likelihood-ratio weights w introduced in 2.3. For the leave-one-out weight vectors that are of primary interest for approximating the jackknife+ and related methods with influence functions, for ease of notation we say that $\tilde{\omega} = -i$ denotes the all ones vector except with zero in the i-th component so that $\widehat{\mu}_{-i}$ still denotes the leave-one-out retrained model, and we denote the corresponding leave-one-out parameters as $\hat{\theta}_{-i} = \hat{\theta}(-i)$.

For any specific weights $\tilde{\omega}$, influence functions assume that $\hat{\theta}(\tilde{\omega})$ is a local minimum of the objective function, and thus that $\hat{\theta}(\tilde{\omega})$ is the solution to the following system of equations, where G is the gradient of the objective function with respect to the model parameters:

$$\hat{\theta}(\tilde{\omega}) := \theta \text{ such that } G(\theta, \tilde{\omega}) := \frac{1}{n}\Big(g_0(\theta) + \sum_{i=1}^{n} \tilde{\omega}_i g_i(\theta)\Big) = 0, \tag{9}$$

where $g_i(\theta)$ is the gradient of the objective function for datapoint i and $g_0(\theta)$ is a prior or regularization term. For the predictor $\widehat{\mu} = \widehat{\mu}_{1_n}$ trained on the full, original dataset, we have $\tilde{\omega} = 1_n$ and can thus denote the model parameters for $\widehat{\mu}$ as $\hat{\theta} = \hat{\theta}(1_n)$. For a resampling-based uncertainty quantification method like the jackknife+ (or bootstrap, cross validation, or other jackknife methods), retraining the model for each new reweighting of the training data can sometimes be computationally burdensome or prohibitive. In these cases, we can instead estimate $\hat{\theta}(\omega)$ using influence functions to compute a Taylor series expansion in ω centered at 1_n (or more specifically a Von Mises expansion, see Fernholz [2012]). A first-order influence function—which we will denote as $\delta_\omega^1 \hat{\theta}(1_n)$ for consistency with notation in Giordano et al. [2019b]—refers to the first-order directional derivative of the parameters $\hat{\theta}(\omega)$ with respect to the weights ω:

$$\delta_\omega^1 \hat{\theta}(1_n) = \sum_{i=1}^{n} \frac{\partial \hat{\theta}(\omega)}{\partial \omega_i}\bigg|_{\omega = 1_n} \Delta\omega_i, \tag{10}$$

where $\Delta\omega = \omega - 1_n$ is the direction of change in weights relative to the original weights 1_n. The first-order influence function $\delta_\omega^1 \hat{\theta}(1_n)$ thus enables a first-order Taylor series approximatinon of $\hat{\theta}(\omega)$, given by

$$\hat{\theta}^{\text{IF-1}}(\omega) := \hat{\theta}(1_n) + \delta_\omega^1 \hat{\theta}(1_n). \tag{11}$$

Computing the influence function $\delta_\omega^1 \hat{\theta}(1_n)$ requires differentiation through the chain rule because $\hat{\theta}(\omega)$ is only implicitly a function of ω through estimating equation 9. The first-order Taylor series approximation of $\hat{\theta}(\omega)$ given in 11 can then be rewritten as

$$\hat{\theta}^{\text{IF-1}}(\omega) := \hat{\theta}(1_n) - \hat{H}(\hat{\theta})^{-1} G(\hat{\theta})(w - 1_n). \tag{12}$$

where $\hat{H}(\hat{\theta}) = \hat{H}(\hat{\theta}(1_n), 1_n)$ and $G(\hat{\theta}) = G(\hat{\theta}(1_n), 1_n)$ are the Hessian and the gradient of the objective function.

Similarly, higher-order Taylor series approximations of $\hat{\theta}(\omega)$ can be obtained using higher order influence functions $\delta_\omega^k \hat{\theta}(1_n)$, where the K-th order Taylor series is given by

$$\hat{\theta}^{\text{IF-}K}(\omega) := \hat{\theta}(1_n) + \sum_{k=1}^{K} \frac{1}{k!} \delta_\omega^k \hat{\theta}(1_n). \tag{13}$$

Computing $\hat{\theta}^{\text{IF-K}}(\omega)$ requires several assumptions. See Giordano et al. [2019b] for a formal list, but informally we assume that $\hat{\theta}(1_n)$ is the solution to $G(\hat{\theta}(1_n), 1_n) = 0$, that $G(\theta, 1_n)$ is $K+1$ times continuously differentiable, that the hessian $H(\hat{\theta})$ is strongly positive definite (meaning that the objective function is strongly convex in the neighborhood of the local solution), and the norm of the derivative $d_\theta^k G(\theta, 1_n)$ has a finite upper bound for $1 \leq k \leq K+1$. In this work, we implement the recursive procedure based on forward-mode automatic differentiation to achieve memory-efficient computation of higher-order directional derivatives Maclaurin et al. [2015] as described in Giordano et al. [2019b].

While Alaa and Van Der Schaar [2020] propose a higher-order IF approximation of the jackknife+, their method assumes exchangeable (e.g., IID) train and test data and offer experiments with only first and second order IF approximations to the jackknife+. Our proposed JAWA sequence extends the IF approximation of the jackknife+ proposed by Alaa and Van Der Schaar [2020] to the setting of covariate shift, and we demonstrate the benefits of this extension on a variety of datasets and orders of influence function approximation.

3 Proposed approach

3.1 JAW: Jackknife+ Weighted with data-dependent weights

We propose adapting the likelihood ratio weighting as in [Tibshirani et al., 2019] to the jackknife+ from [Barber et al., 2021]. While the coverage results of [Tibshirani et al., 2019] extend split and full conformal prediction to their corresponding weighted versions, it is not trivial to see that the same is true for the jackknife+ (see Section 4.1 Remarks). We first present the main result before discussing the implications.

We present JAW, the weighted jackknife+ predictive interval with data-dependent, normalized likelihood-ratio weights:

$$\begin{aligned} \widehat{C}_{n,\alpha}^{\text{JAW}}(X_{n+1}) = \Big[& \widehat{q}^{-}_{n,\alpha}\big\{p_i^w(X_{n+1}) \cdot \delta_{\widehat{\mu}_{-i}(X_{n+1}) - R_i^{LOO}}\big\}, \\ & \widehat{q}^{+}_{n,\alpha}\big\{p_i^w(X_{n+1}) \cdot \delta_{\widehat{\mu}_{-i}(X_{n+1}) + R_i^{LOO}}\big\}\Big] \end{aligned} \tag{14}$$

where $R_i^{LOO} = \big|\widehat{\mu}_{-i}(X_i) - Y_i\big|$, and where we use $\widehat{q}^{+}_{n,\alpha}\big\{p_i^w(X_{n+1}) \cdot \delta_{\widehat{\mu}_{-i}(X_{n+1}) + R_i^{LOO}}\big\}$ to denote the level $1-\alpha$ of the empirical distribution $\sum_{i=1}^{n} \big[p_i^w(X_{n+1}) \cdot \delta_{\widehat{\mu}_{-i}(X_{n+1}) + R_i^{LOO}}\big] + p_{n+1}^w(X_{n+1}) \cdot \delta_\infty$ and $\widehat{q}^{-}_{n,\alpha}\big\{p_i^w(X_{n+1}) \cdot \delta_{\widehat{\mu}_{-i}(X_{n+1}) - R_i^{LOO}}\big\}$ to denote the level α quantile of the empirical distribution $\sum_{i=1}^{n} \big[p_i^w(X_{n+1}) \cdot \delta_{\widehat{\mu}_{-i}(X_{n+1}) - R_i^{LOO}}\big] + p_{n+1}^w(X_{n+1}) \cdot \delta_{-\infty}$. Here, the $p_i^w(X)$ is the normalized likelihood ratio weights as defined in (3).

When oracle likelihood ratio weights are not available as is often the case in practice, the likelihood ratios can be estimated through an approach such as probabilistic classification, moment matching, or minimization of ϕ-divergences (for a review of likelihood ratio estimation approaches see Sugiyama et al. [2012]). When estimated rather than oracle likelihood ratios are used, the performance of the JAW predictive interval will depend on the quality of the likelihood ratio estimate, and thus we refer to JAW with estimated weights with the modified name JAW-E to take note of this difference.

3.2 JAWA: Jackknife+ Weighted with data-dependent weights Approximation

To provide a computationally efficient approximation to JAW that avoids retraining n leave-one-out models, we propose the JAWA sequence, which approximates the leave-one-out models required by JAW using higher-order influence functions. Let $\hat{\theta}$ denote the original model parameters for a given fitted model $\widehat{\mu}$, and let $\hat{\theta}_{-i}$ denote the fitted model parameters for $\widehat{\mu}_{-i}$ that would be obtained

by retraining the model on $\{(X_1, Y_1), ..., (X_{i-1}, Y_{i-1}), (X_{i+1}, Y_{i+1}), ..., (X_n, Y_n)\}$ (or equivalent, by reweighting point (X_i, Y_i) with weight $\omega_i = 0$ and retraining).

For each training point $i \in \{1, ..., n\}$, define the K-th order influence function approximation to the leave-one-out refit parameters $\hat{\theta}_{-i}$, obtained from Algorithm 4 in Giordano et al. [2019b], as

$$\hat{\theta}_{-i}^{\text{IF-}K} := \hat{\theta}(1_n) + \sum_{k=1}^{K} \frac{1}{k!} \delta_\omega^k \hat{\theta}(1_n), \tag{15}$$

and let $\widehat{\mu}_{-i}^{\text{IF-}K}$ be the model with with these approximated parameters $\hat{\theta}_{-i}^{\text{IF-}K}$ for each $i \in \{1, ..., n\}$. Then, the K-th order JAWA prediction interval (i.e., for JAWA-K) is given by

$$\begin{aligned}\widehat{C}_{n,\alpha}^{\text{JAWA-}K}(X_{n+1}) = \Big[&\widehat{q}^{-}_{n,\alpha}\big\{p_i^w(X_{n+1}) \cdot \delta_{\widehat{\mu}_{-i}^{\text{IF-}K}(X_{n+1}) - R_i^{\text{IF-}K,LOO}}\big\}, \\ &\widehat{q}^{+}_{n,\alpha}\big\{p_i^w(X_{n+1}) \cdot \delta_{\widehat{\mu}_{-i}^{\text{IF-}K}(X_{n+1}) + R_i^{\text{IF-}K,LOO}}\big\}\Big]\end{aligned} \tag{16}$$

where $R_i^{\text{IF-}K,LOO} = \big|\widehat{\mu}_{-i}^{\text{IF-}K}(X_i) - Y_i\big|$, where the quantiles are defined analogously as in the definition for JAW, and where $p_i^w(X)$ still denotes the normalized likelihood ratio weights as defined in (3).

3.3 Risk assessment for exchangeable data

We now propose a general approach to adapting any predictive inference method and its coverage guarantee for exchangeable data to the task of risk assessment, that is, estimating the probability that a true test point label Y_{n+1} lies within a given arbitrary, finite interval $I = [a_L, a_U]$. The key idea is to leverage a predictive inference method's predictive *distribution* (from which predictive intervals are obtained for a given coverage guarantee) to find the method's largest predictive interval contained within I, and then to use the target coverage of this largest predictive sub-interval to estimate the coverage of I.

Given a predictive inference uncertainty auditing method for generating intervals $\widehat{C}_{n,\alpha}^{\text{audit}}(X_{n+1}) = \big[q^{-}_{n,\alpha}\{\frac{1}{n+1}\delta_{V_i^L}\},\ q^{+}_{n,\alpha}\{\frac{1}{n+1}\delta_{V_i^U}\}\big]$ that satisfy the coverage requirement $\mathbb{P}\{Y_{n+1} \in \widehat{C}_{n,\alpha}^{\text{audit}}(X_{n+1})\} \geq 1 - c_1\alpha - c_2$ for exchangeable train and test data where $c_1, c_2 > 0$ are constants, suppose we are given some arbitrary interval $I = [a_L, a_U] \subseteq \mathbb{R}$ (assuming $a_L \leq a_U$ WLOG) whose coverage we are interested in estimating. Define α_I^{audit} as follows:

$$\alpha_I^{\text{audit}} = \min\left(\left\{\alpha' \,:\, a_L \leq q^{-}_{n,\alpha'}\Big\{\frac{1}{n+1}\delta_{V_i^L}\Big\},\ q^{+}_{n,\alpha'}\Big\{\frac{1}{n+1}\delta_{V_i^U}\Big\} \leq a_U\right\}\right). \tag{17}$$

Then, we estimate the coverage probability for interval I as the predictive inference method's target coverage for the interval corresponding to α_I^{audit}:

$$\widehat{p}\{Y_{n+1} \in I\} = \begin{cases} 1 - \alpha_I^{\text{audit}} & \text{if } \alpha_I^{\text{audit}} \text{ exists} \\ 0 & \text{otherwise} \end{cases} \tag{18}$$

Note that the target coverage $1 - \alpha_I^{\text{audit}}$ is used as the estimator rather than the guarantee of $1 - c_1\alpha_I^{\text{audit}} - c_2$ because empirically, the jackknife+ and similar methods with guarantees below the target coverage level (e.g., cross validation+) typically still perform approximately at the target level when the exchangeability assumption is met Barber et al. [2021]. Figure 2 illustrates the terms involved in computing α_I^{audit}. Note that for standard conformal prediction methods, the values $\{V_i^L\}$ and $\{V_i^U\}$ are symmetric about the original prediction $\widehat{\mu}(X_{n+1})$: for either split or full conformal prediction methods with nonconformity scores R_i, $V_i^L = \widehat{\mu}(X_{n+1}) - R_i$ and $V_i^U = \widehat{\mu}(X_{n+1}) + R_i$ for all $i \in \{1, ..., n\}$. On the other hand, for jackknife+ we instead have $V_i^L = \widehat{\mu}_{-i}(X_{n+1}) - R_i^{LOO}$ and $V_i^U = \widehat{\mu}_{-i}(X_{n+1}) + R_i^{LOO}$ for all $i \in \{1, ..., n\}$, and the values $\{V_i^L\}$ and $\{V_i^U\}$ are in general are not symmetric about the original prediction.

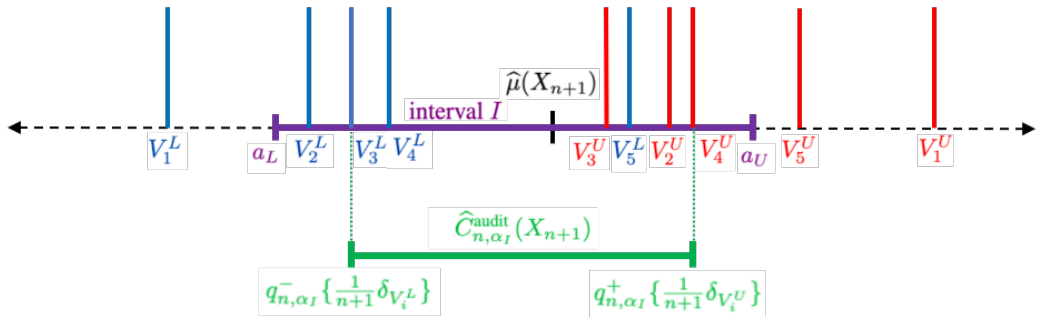

Figure 2: Illustration of terms involved in computing α_I^{audit}. The interval $I = [a_L, a_U]$ is shown in violet, the values $\{V_i^L\}$ in blue, the values $\{V_i^U\}$ in red, and the interval $\widehat{C}^{\text{audit}}_{n,\alpha}(X_{n+1})$ in green. Each vertical line at a location V_i on the real line represents a point mass δ_{V_i} with height $\frac{1}{n+1}$.

3.4 Risk assessment under covariate shift

We next propose a more general risk assessment approach that relaxes the assumption of data exchangeability to allow for possible covariate shift. This approach also encompasses the repurposing of JAW and JAWA to risk assessment (which we refer to JAW-R and JAWA-R respectively). The goal for our general approach remains the same of estimating the probability that a true test point lies within a given arbitrary, finite interval $I = [a_L, a_U]$. The key idea of leveraging the method's largest predictive interval contained within I is also the same as in the exchangeable data case.

Given a predictive inference method for generating intervals $\widehat{C}^{\text{audit}}_{n,\alpha}(X_{n+1}) = \left[q^-_{n,\alpha}\{p_i^w(x)\delta_{V_i^L}\},\ q^+_{n,\alpha}\{p_i^w(x)\delta_{V_i^U}\}\right]$ with coverage guarantee $\mathbb{P}\{Y_{n+1} \in \widehat{C}^{\text{audit}}_{n,\alpha}(X_{n+1})\} \geq 1 - c_1\alpha - c_2$ under covariate shift where $c_1, c_2 \geq 0$ are constants, suppose we are given some arbitrary interval $I = [a_L, a_U] \subseteq \mathbb{R}$ (assuming $a_L \leq a_U$ WLOG) whose coverage we are interested in estimating. Define $\alpha_I^{\text{w-audit}}$ as follows:

$$\alpha_I^{\text{w-audit}} = \min\left(\left\{\alpha' \ :\ a_L \leq\ q^-_{n,\alpha'}\{p_i^w(x)\delta_{V_i^L}\}\ ,\ q^+_{n,\alpha'}\{p_i^w(x)\delta_{V_i^U}\} \leq a_U\right\}\right). \tag{19}$$

Then, we estimate the coverage probability for interval I as the predictive inference method's target coverage for the interval corresponding to $\alpha_I^{\text{w-audit}}$:

$$\widehat{p}\{Y_{n+1} \in I\} \geq \begin{cases} 1 - \alpha_I^{\text{w-audit}} & \text{if } \alpha_I^{\text{w-audit}} \text{ exists} \\ 0 & \text{otherwise} \end{cases}. \tag{20}$$

As in the proposed risk assessment approach for exchangeable data, the proposed approach for the covariate shift setting uses the target coverage $1 - \alpha_I^{\text{w-audit}}$ as the estimator rather than the worst case guarantee because empirically, JAW typically performs at the target level despite covariate shift (as we will see in Figure 6) and JAWA typically performs at or close to the target level (Figure 7). Figure 3 illustrates the terms involved in computing $\alpha_I^{\text{w-audit}}$. The values involved in computing $\alpha_I^{\text{w-audit}}$ are the same as those for computing α_I^{audit}, except obtaining $\alpha_I^{\text{w-audit}}$ also requires the data-dependent likelihood ratio weights $p_i^w(x)$. We describe the process of computing α_I^{JAW} as JAW-R and similarly to the process of computing $\alpha_I^{\text{JAWA-}K}$ as JAWA-R-K.

4 Theoretical results

4.1 JAW predictive interval finite sample coverage guarantee

We show that $\widehat{C}^{\text{JAW}}_{n,\alpha}(X_{n+1})$ satisfies a coverage guarantee identical to that of the unweighted jackknife+ except with the data exchangeability assumption relaxed to allow for covariate shift, which we state formally in the following theorem:

Theorem 1. *With covariate shift between the training and test data, the JAW interval in* (14) *satisfies*

$$\mathbb{P}\{Y_{n+1} \in \widehat{C}^{\text{JAW}}_{n,\alpha}(X_{n+1})\} \geq 1 - 2\alpha \tag{21}$$

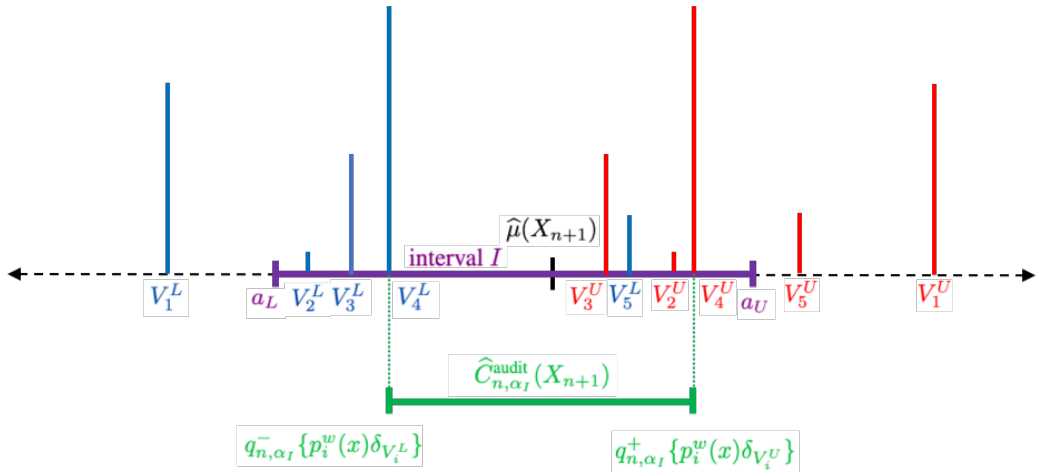

Figure 3: Illustration of terms involved in computing $\alpha_I^{\text{w-audit}}$. The interval $I = [a_L, a_U]$ is shown in violet, the values $\{V_i^L\}$ in blue, the values $\{V_i^U\}$ in red, and the interval $\widehat{C}^{\text{audit}}_{n,\alpha}(X_{n+1})$ in green. Each vertical line at a location V_i on the real line represents a point mass δ_{V_i} with height corresponding to the normalized likelihood ratio weight $p_i^w(x)$. Note that Figure 2 and Figure 3 have the same values $\{V_i^L\}$ and $\{V_i^U\}$, but that the resulting green sub-interval is different due to the presence of the normalized likelihood ratio weights $p_i^w(x)$.

Remarks: We leave the proof to the Appendix A.1, but emphasize the implication of the theorem. This guarantee extends the jackknife+ coverage guarantee to the setting of covariate shift, similarly to how the weighted conformal prediction framework [Tibshirani et al., 2019] extends standard conformal prediction to covariate shift. However, we highlight two significant differences in deriving Theorem 1 for JAW, when compared to deriving the analogous result for weighted standard conformal prediction in Tibshirani et al. [2019]:

1. Non-existence of nonconformity scores: The standard conformal prediction depends on a score function $\mathcal{S}$ and corresponding nonconformity scores $\{V_i\}$, but the Jackknife+ has neither. For split and full conformal prediction, the results from [Tibshirani et al., 2019] directly apply because weighted exchangeability of the nonconformity scores $\{V_1, ..., V_n, V_{n+1}\}$ allow one to assume that V_{n+1} is as likely to lie outside of $q^+_{n,\alpha}\{p_i^w(x)\delta_{V_i}\}$ as any other nonconformity score V_i. However, the jackknife+ does not have nonconformity scores that we can directly apply this result to.
2. Non-existence of weighted exchangeability for the leave-one-out models: Even without nonconformity scores, the approach analogous to that of Tibshirani et al. [2019] for the jackknife+ would be to assume that $\{\widehat{\mu}_{-i}(X_{n+1}) + R_i^{LOO}\}$ is weighted exchangeable for $i \in \{1, ..., n+1\}$ (and same for $\{\widehat{\mu}_{-i}(X_{n+1}) + R_i^{LOO}\}$). However, observe that for $i \in \{1, ..., n\}$, $\widehat{\mu}_{-i}$ is trained on $n-1$ datapoints, whereas $\widehat{\mu}_{-(n+1)} = \widehat{\mu}$ is trained on n datapoints. Thus, $\widehat{\mu}_{-i}$ and $\widehat{\mu}_{-(n+1)}$ differ beyond a mere reweighting, and therefore $\widehat{\mu}_{-i}(X_{n+1}) + R_i^{LOO}$ and $\widehat{\mu}_{-(n+1)}(X_{n+1}) + R_{n+1}^{LOO}$ are not weighted exchangeable. As we will see in the proof sketch, extending weighted conformal prediction to the jackknife+ requires that we treat each $\widehat{\mu}_{-i}$ as the leave-*two*-out model $\widehat{\mu}_{-(i,n+1)}$ as in Barber et al. [2021].

Proof sketch: Our proof technique follows the approach of Barber et al. [2021], and it adapts weighted conformal prediction as described in Tibshirani et al. [2019] to the jackknife+ method. It can also be viewed as generalizing the proof in Barber et al. [2021] to the covariate shift setting with likelihood ratio weights. The outline is as follows:

1. *Setup*: Following Barber et al. [2021], we suppose access to the test point (X_{n+1}, Y_{n+1}) and define a set of leave-*two*-out models $\{\tilde{\mu}_{-(i,j)}\}$ (where $\tilde{\mu}$ rather than $\widehat{\mu}$ reminds us that the former may be fit with access to the test point). We then generalize the notion of "strange" or hard-to-predict points described in Barber et al. [2021] to the covariate shift setting.
2. *Bounding the total normalized weight of strange points*: We establish deterministically that the total normalized weight of strange points cannot exceed 2α.

3. *Weighted exchangeability using the leave-two-out models*: Using the leave-two-out model construction, we are able to leverage weighted exchangeability to show that the probability that a test point $n+1$ is strange is thus bounded by 2α.
4. *Connection to JAW*: Lastly, we show that the JAW interval can only fail to cover the test label value Y_{n+1} if $n+1$ is a strange point.

4.2 JAWA predictive interval asymptotic coverage guarantee

We now provide an asymptotic coverage guarantee for $\widehat{C}^{\text{JAWA-}K}_{n,\alpha}(X_{n+1})$ that holds either in the limit of the sample size or in the limit of the influence function order, under regularity conditions formally described in Giordano et al. [2019b]. These assumptions concern the regularity of the training data, local convexity of the objective's Hessian, and boundedness of the objective's higher-order derivatives.

Theorem 2. *Let Assumptions 1 - 4 and either Condition 2 or Condition 4 from Giordano et al. [2019b] hold uniformly for all n. Then, with covariate shift between the training and test data, in either the limit of the training sample size $n \to \infty$ or in the limit of the influence function order $K \to \infty$, the JAWA-K interval in* (16) *satisfies*

$$\mathbb{P}\{Y_{n+1} \in \widehat{C}^{\textit{JAWA-}K}_{n,\alpha}(X_{n+1})\} \geq 1 - 2\alpha \tag{22}$$

We leave the proof to Appendix A.2, but the result follows by combining Propositions 2 and 3 in Giordano et al. [2019b] with our Theorem 1 stated above.

4.3 Risk assessment guarantee with exchangeable data

We now present the guarantee for our risk assessment approach assuming exchangeable data. Whereas the approach presented in Section 3.3 was based on empirical coverage performance of a predictive inference auditing method at the target coverage level, our guarantee provides the worst-case coverage for an arbitrary finite interval I. Note that δ_{V_i} denotes a point mass at some value V_i.

Theorem 3. *Given a predictive inference method for generating intervals $\widehat{C}^{\textit{audit}}_{n,\alpha}(X_{n+1}) = \left[q^{-}_{n,\alpha}\{\frac{1}{n+1}\delta_{V_i^L}\},\ \ q^{+}_{n,\alpha}\{\frac{1}{n+1}\delta_{V_i^U}\}\right]$ that satisfy the coverage requirement $\mathbb{P}\{Y_{n+1} \in \widehat{C}^{\textit{audit}}_{n,\alpha}(X_{n+1})\} \geq 1 - c_1\alpha - c_2$ for exchangeable train and test data where $c_1, c_2 > 0$ are constants, suppose we are given some arbitrary interval $I = [a_L, a_U] \subseteq \mathbb{R}$ (assuming $a_L \leq a_U$ WLOG) whose coverage we are interested in estimating. Define α_I as follows:*

$$\alpha_I^{\textit{audit}} = \min\left(\left\{\alpha' \,:\, a_L \leq\ q^{-}_{n,\alpha'}\left\{\frac{1}{n+1}\delta_{V_i^L}\right\},\ q^{+}_{n,\alpha'}\left\{\frac{1}{n+1}\delta_{V_i^U}\right\} \leq a_U\right\}\right). \tag{23}$$

Then, I has coverage given by

$$\mathbb{P}\{Y_{n+1} \in I\} \geq \begin{cases} 1 - c_1\alpha_I^{\textit{audit}} - c_2 & \textit{if } \alpha_I \textit{ exists and } \alpha_I^{\textit{audit}} < \frac{1-c_2}{c_1} \\ 0 & \textit{otherwise} \end{cases}. \tag{24}$$

The proof for Theorem 3 is given in Appendix A.3.

4.4 Risk assessment guarantee under covariate shift

The following theorem generalizes Theorem 2 for an arbitrary predictive inference method with data-dependent normalized likelihood ratio weights $p_i^w(x)$ with a coverage guarantee under covariate shift (e.g., weighted standard conformal prediction or JAW). Thus, whereas Section 3.4 presents presents an estimate of the coverage for a given finite interval I based on empirical performance of a predictive inference auditing method at the target coverage level, the following theorem presents a worse-case guarantee for the same task. Note that δ_{V_i} denotes a point mass at some value V_i.

Theorem 4. *Given a predictive inference method for generating intervals $\widehat{C}^{\textit{audit}}_{n,\alpha}(X_{n+1}) = \left[q^{-}_{n,\alpha}\{p_i^w(x)\delta_{V_i^L}\},\ q^{+}_{n,\alpha}\{p_i^w(x)\delta_{V_i^U}\}\right]$ with coverage guarantee $\mathbb{P}\{Y_{n+1} \in \widehat{C}^{\textit{audit}}_{n,\alpha}(X_{n+1})\} \geq$*

$1 - c_1\alpha - c_2$ *under covariate shift where* $c_1, c_2 > 0$ *are constants, suppose we are given some arbitrary interval* $I = [a_L, a_U] \subseteq \mathbb{R}$ *(assuming* $a_L \leq a_U$ *WLOG) whose coverage we are interested in estimating. Define* $\alpha_I^{\textit{audit}}$ *as follows:*

$$\alpha_I^{\textit{w-audit}} = \min\left(\left\{\alpha' \,:\, a_L \leq q^-_{n,\alpha'}\{p_i^w(x)\delta_{V_i^L}\}\,,\; q^+_{n,\alpha'}\{p_i^w(x)\delta_{V_i^U}\} \leq a_U\right\}\right). \tag{25}$$

Then, I *has coverage given by*

$$\mathbb{P}\{Y_{n+1} \in I\} \geq \begin{cases} 1 - c_1\alpha_I^{\textit{audit}} - c_2 & \textit{if } \alpha_I^{\textit{w-audit}} \textit{ exists and } \alpha_I^{\textit{w-audit}} < \frac{1-c_2}{c_1} \\ 0 & \textit{otherwise} \end{cases}. \tag{26}$$

The proof for Theorem 4 is given in Appendix A.4.

We now state the risk assessment guarantee for JAW-R as Corollary 1, which follows directly from Theorem 4 in the covariate shift setting with normalized likelihood ratio weights $p_i^w(x)$ when $V_i^L = \widehat{\mu}_{-i}(X_{n+1}) - R_i^{LOO}$ and $V_i^U = \widehat{\mu}_{-i}(X_{n+1}) + R_i^{LOO}$ for all $i \in \{1, ..., n\}$:

Corollary 1. *Given an arbitrary interval* $I = [a_L, a_U]$*, define*

$$\alpha_I^{JAW} = \min\left(\left\{\alpha' \,:\, a_L \leq q^-_{n,\alpha'}\{p_i^w(x)\delta_{\widehat{\mu}_{-i}(X_{n+1})-R_i^{LOO}}\}\,,\; q^+_{n,\alpha'}\{p_i^w(x)\delta_{\widehat{\mu}_{-i}(X_{n+1})+R_i^{LOO}}\} \leq a_U\right\}\right). \tag{27}$$

Then, I has coverage guarantee given by

$$\mathbb{P}\{Y_{n+1} \in I\} \geq \begin{cases} 1 - 2\alpha_I^{JAW} & \textit{if } \alpha_I^{\textit{JAW}} \textit{ exists and } \alpha_I^{JAW} < \frac{1}{2} \\ 0 & \textit{otherwise} \end{cases} \tag{28}$$

Lastly for our theoretical results, we state the risk assessment guarantee for JAWA-R as Corollary 2. Whereas Corollary 1 holds for finite samples, Corollary 2 holds in the limit either of the number of samples or in the order of the influence function approximation.

Corollary 2. *Let Assumptions 1 - 4 and either Condition 2 or Condition 4 from Giordano et al. [2019b] hold uniformly for all* n*. Given an arbitrary interval* $I = [a_L, a_U]$*, define*

$$\alpha_I^{\textit{JAWA-K}} = \min\left(\left\{\alpha' \,:\, a_L \leq q^-_{n,\alpha'}\{p_i^w(x)\delta_{\widehat{\mu}^{\textit{IF-K}}_{-i}(X_{n+1})-R_i^{\textit{IF-K},LOO}}\}\,, \tag{29}$$

$$q^+_{n,\alpha'}\{p_i^w(x)\delta_{\widehat{\mu}^{\textit{IF-K}}_{-i}(X_{n+1})+R_i^{\textit{IF-K},LOO}}\} \leq a_U\right\}\right). \tag{30}$$

Then, as either $N \to \infty$ *or as* $K \to \infty$*,* I *has coverage guarantee given by*

$$\mathbb{P}\{Y_{n+1} \in I\} \geq \begin{cases} 1 - 2\alpha_I^{\textit{JAWA-K}} & \textit{if } \alpha_I^{\textit{JAWA-K}} \textit{ exists and } \alpha_I^{\textit{JAWA-K}} < \frac{1}{2} \\ 0 & \textit{otherwise} \end{cases} \tag{31}$$

5 Experiments[3]

5.1 Datasets and creation of covariate shift

We conduct experiments on five UCI datasets Dua and Graff [2017] with various numbers of features: airfoil self-noise (airfoil), red wine quality prediction (wine) [Cortez et al., 2009], wave energy converters (wave), superconductivity (superconduct) [Hamidieh, 2018], and communities and crime (communities) [Redmond and Baveja, 2002]. Table 2 shows their statistics.

[3] Additional experimental analysis and a link to code for all experiments and included in Appendix B and C

Table 2: Dataset statistics for the UCI datasets. The full dataset was used for the airfoil, wine, and communities datasets. Only the first 2000 samples were used for the wave and superconductivity datasets (in the case of wave, the first 2000 samples of the Adelaide data were used).

Dataset	# of samples	# of features	label range
Airfoil	1503	5	[103.38, 140.987]
Red wine quality	1599	11	[3, 8]
Wave energy converters	2000	48	[1226969, 1449349]
Superconductivity	2000	81	[0.2, 136.0]
Communities and crime	1994	99	[0, 1]

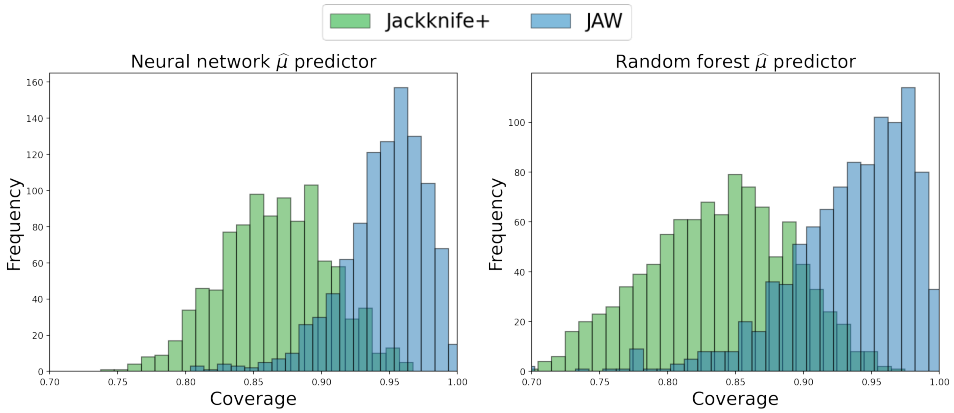

Figure 4: Comparison of the histogram of coverage on Airfoil under covariate shift, when $\beta = (-1, 0, 0, 0, 1)$. JAW still achieves high coverage while jackknife+ loses coverage significantly. This is 1000 replicates of the experiments.

For the creation of covariate shift, we use a similar exponential tilting procedure as in [Tibshirani et al., 2019] to induce covariate shift on the test data. In particular, we first randomly split the data into two portions. The first portion is used for training and consisted of 200 samples in all experiments. The test distribution is then sampled from the remaining datapoints that are not used for training with probabilities proportional to exponential tilting weights, thus producing a biased test set with total number of test points equal to half the number of points not used for training.

For the relatively lower dimensional airfoil and wine datasets, the weights took the form $w(x) = \exp(x^T\beta)$. For the relatively higher dimensional wave, superconductivity, and communities datasets, the weights took the form $w(x) = \exp(x_{\text{PCA}}^T\beta)$ where x_{PCA} is some PCA-based representation of the covariates data x. We can tune β to generate different magnitudes of covariate shift. Figure 5 shows the distribution first and last features in the airfoil dataset before and after the exponential tilting is applied to induce covariate shift with parameter $\beta = (-1, 0, 0, 0, 1)$. In our main experiments, exponential tilting parameters were selected for each dataset so that the associated covariate shift would result in a similar loss in how informative the training set is regarding the biased test set, as assess by reduced effective sample size (see Appendix B.1 for more details on the creation of covariate shift).

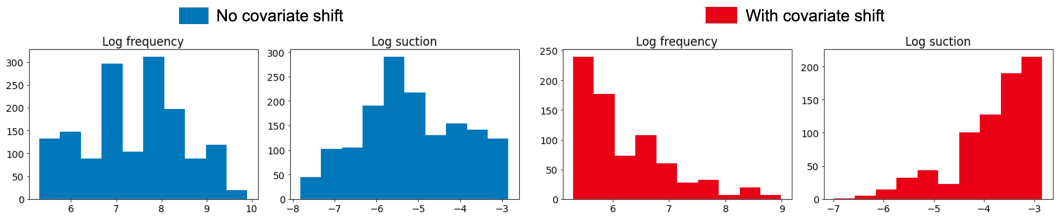

Figure 5: Distribution log frequency and log suction features of airfoil dataset before and after exponential tilting.

5.2 Baselines

Baselines for comparison to JAW We compared the proposed JAW method to the following baselines:

1. **Naive** method uses the residuals on the training data, $|Y_i - \widehat{\mu}(X_i)|$, to estimate the typical prediction error on the new test point. This method usually suffers from overfitting, which may be even worse under covariate shift.
2. **Jackknife** uses the classic Jackknife resampling as in (6).
3. **Jackknife+** follows (7) that replaces the prediction $\widehat{\mu}(X_{n+1})$ in jackknife with $\widehat{\mu}_{-i}(X_{n+1})$, which is the predictor trained using ith datapoint removed.
4. **CV+** (cross validation) splits the data into K portions and replaces the $\widehat{\mu}_{-i}(X_{n+1})$ with $\widehat{\mu}_{-k}(X_{n+1})$, which is the model trained with the kth subset removed. Jackknife+ can be viewed as the special case of CV+ when $K = n$.
5. **Split** method follows the split conformal prediction and use half of the data for training and the other half of the data for generating the nonconformal scores.
6. **Jackknife-mm** method is a more conservative alternative to the jackknife+ method. In the IID setting, it always achieves the target coverage rate $1 - \alpha$ but usually produces overly-wide confidence intervals.

$$\widehat{C}^{\text{jackknife-mm}}_{n,\alpha}(X_{n+1}) = \Big[\min_{i=1,\ldots,n} \widehat{\mu}_{-i}(X_{n+1}) - \widehat{q}^{+}_{n,\alpha}\{R^{LOO}_i\}, \max_{i=1,\ldots,n} \widehat{\mu}_{-i}(X_{n+1}) + \widehat{q}^{+}_{n,\alpha}\{R^{LOO}_i\}\Big] \tag{32}$$

Baselines for comparison to JAWA For influence function orders $K \in \{1, 2, 3\}$, we compared the proposed JAWA-K method with K-th order influence function approximations of the jackknife-based baselines that we used as comparisons to JAW. Each baseline compared to JAWA-K is thus also approximated with the same K-th order leave-one-out influence function models.

1. **IF-*K* Jackknife** Approximation of the classic jackknife using K-th order influence functions to approximate each leave-one-out residual R^{LOO}_i in (6) (which require $\widehat{\mu}_{-i}(X_i)$ predictions to compute).
2. **IF-*K* Jackknife+** Approximation of the jackknife+ using K-th order influence functions to approximate the $\widehat{\mu}_{-i}(X_i)$ predictions as well as the leave-one-out residuals R^{LOO}_i in (7).
3. **IF-*K* Jackknife-mm** Approximation of the jackknife-mm using K-th order influence functions to approximate the $\widehat{\mu}_{-i}(X_i)$ predictions as well as the leave-one-out residuals R^{LOO}_i in (32).

5.3 Models

For all experiments involving JAW and its baselines, we standardize the training data size across datasets by randomly sampling 200 data points from the full dataset to use as the training data. The test points are then sampled from the remaining points using exponential-tilting covariate shift such that the total number of test points is equal to half the number of points not used for training. We run the experiments involving JAW and its baselines using two different regression algorithms: random forests (scikit-learn RandomForestRegressor), and neural networks (scikit-learn MLPRegressor with LBFGS optimizer, logistic activation, and default parameters otherwise) as our predictor $\widehat{\mu}$.

For all experiments comparing the coverage and interval width of JAWA to other influence function approximated baselines, we used a neural network predictor with one hidden layer consisting of 25 hidden units. Covariate and label data were centered and scaled, and 200 samples were used for training in all experiments. The neural network was trained for 2000 epochs with batch sizes of 50 and a learning rate of 0.0001, which generally resulted in convergence. The objective function for the neural network in JAWA is the negative log likelihood with a Gaussian prior or L2 regularization term. The L2 regularization term was included in the objective function due to assumptions in Giordano et al. [2019b] required for theoretically bounding the error in the influence function estimates as well as due to recent empirical findings of first-order influence functions in neural networks requiring weight-decay regularization for reliable results. The λ L2-regularization parameter was tuned using a grid search prior to all experiments using a "tuning" validation set of 200 samples that were excluded from both the training and test sets in the experiments (see Appendix B.2 for more details regarding the L2 regularization tuning).

5.4 Experimental results

5.4.1 Interval-generating audit experiments: coverage and interval width

This set of experiments focus on evaluating the empirical coverage and predictive interval width for JAW compared to jackknife+ and other baselines on all five UCI datasets under covariate shift. Figure 6 demonstrates the performance comparison of JAW and its baselines for 200 experimental replicates on each dataset and predictor function, firstly regarding mean predictive interval coverage, and secondarily regarding median interval width.

Meeting the target coverage level of $1 - \alpha$ is the primary goal of the interval-generation audit task, so the first indication of a good method is whether the mean coverage reaches this target coverage level ($1 - \alpha = 0.9$ noted by the dashed line in Figure 6). Then, for a method that meets or nearly meets the target coverage level, smaller interval widths are more informative than larger interval widths. In other words, an interval that achieves target coverage and small width is ideal, an interval with low coverage and small width is misleading, and any interval with overly large width can be uninformative in practice (e.g., $\mathbb{R}$ trivially has coverage of 1.0 but conveys no information). The definition of an "overly large" interval width may depend on a task- and dataset-specific decomposition decomposition of predictive uncertainty into epistemic (reducible) and aleatoric (unreducible) uncertainty, where the most informative predictive intervals would represent only aleatoric uncertainty and no epistemic uncertainty.

As seen in Figure 6, the JAW predictive interval coverage is above the target level of 0.9 across all datasets, for both random forest and neural network $\widehat{\mu}$ functions. In each of these conditions, JAW has higher coverage than the jackknife+ and all other baselines aside from jackknife-mm, but JAW's interval widths are generally smaller and thus more informative than those of jackknife-mm (which are often overly large, as noted in Barber et al. [2021]). Figure 4 also demonstrates an example histogram comparison between JAW and jackknife+. JAW maintains the high coverage under covariate shift.

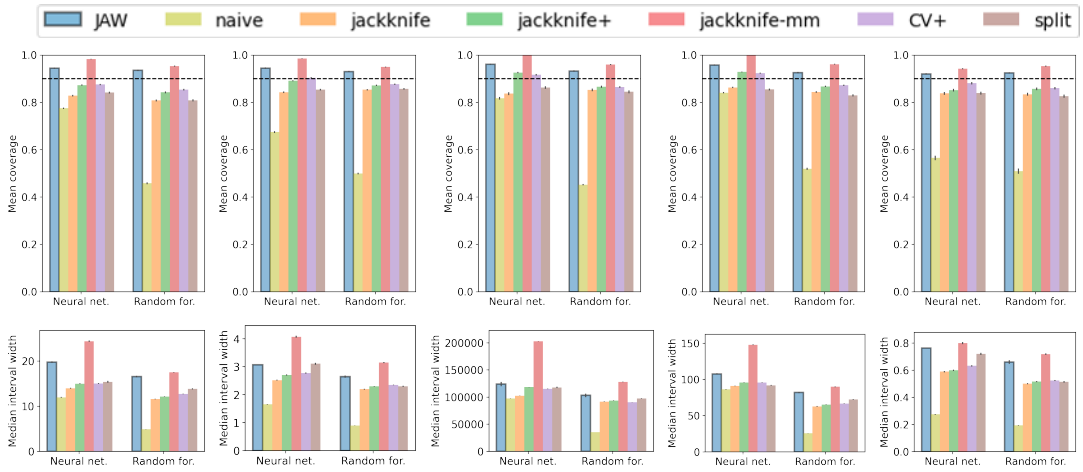

(a) Airfoil (b) Wine (c) Wave (d) Superconduct (e) Communities

Figure 6: Mean coverage (first row) and median interval width (second row) comparison for neural network and random forest predictors on the UCI datasets. Dashed line is the target coverage level ($1 - \alpha = 0.9$). JAW achieves the target coverage with much lower width of confidence interval than the other method that does the same (jackknife-mm). Error bar shows the standard error of 200 repeated experiments.

5.4.2 JAWA coverage and interval width experiments

In this set of experiments, we evaluate the empirical coverage and predictive interval for JAWA. The setup is the same as in the JAW experiments. Figure 7 evaluates the performance of JAWA for influence function orders $K \in \{1, 2, 3\}$ with other K-th order influence function approximations of jackknife-based methods as baselines. As with the main JAW coverage and interval width experiments,

coverage at the target level of $1 - \alpha = 0.9$ is the primary goal, while secondarily, smaller intervals are more informative so long as a method's coverage meets or nearly meets the target threshold. Across all three of five datasets (airfoil, wine, and communities) JAWA is the only method that consistently reaches or nearly reaches the target coverage level for all tested influence function orders. In the wave dataset, JAWA as well as all of the baselines reach the target coverage level, while in the superconduct dataset JAWA still outperforms approximations of the jackknife and jackknife+ for all influence function orders.

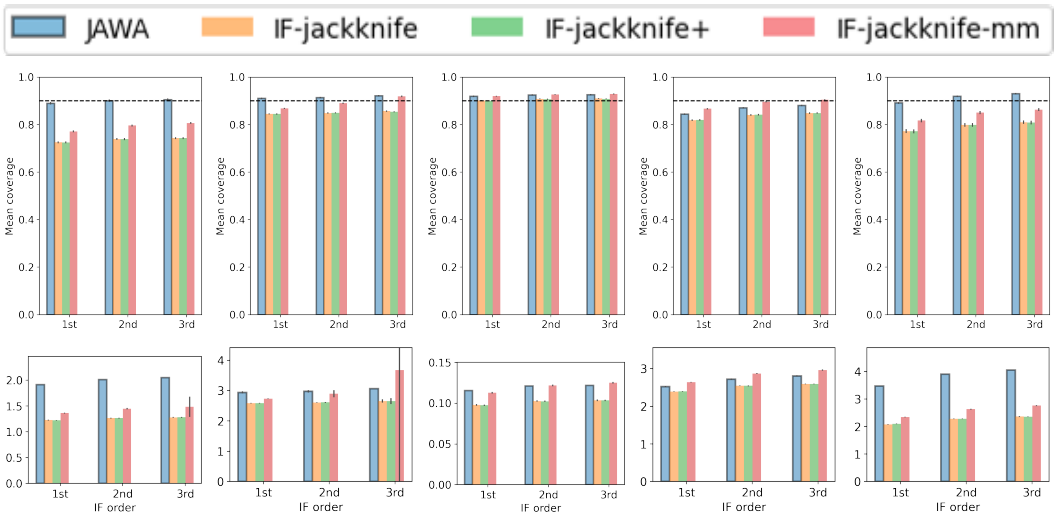

(a) Airfoil (b) Wine (c) Wave (d) Superconduct (e) Communities

Figure 7: Mean coverage (first row) and median interval width (second row) comparison JAWA compared to jackknife-based approximation baselines for first, second, and third order influence functions. Dashed line is the target coverage level ($1 - \alpha$ = 0.9). JAWA achieves the most consistent coverage compared to the baselines across all influence function orders and across most datasets. Error bar shows the standard error of 200 repeated experiments.

5.4.3 Empirical runtime of JAWA compared to JAW

Whereas JAW requires retraining n leave-one-out models, JAWA does not require any retraining, and thus generally enjoys significantly faster runtime than JAW. In the following table we report the empirical runtime of JAW compared to JAWA for different orders of JAWA's influence function approximation. In these experiments, JAWA is orders of magnitude faster than JAWA regardless of whether the influence function approximation is first, second, or third order (though of course the specific runtime statistics depend on the model architecture, optimization scheme, or dataset). JAWA's runtime does not increase substantially (relative to JAW's runtime) with increased influence function orders for $K \in \{1, 2, 3\}$.

Table 3: Example empirical comparison between the runtime for JAW and JAWA-K for different influence function approximation orders $K \in \{1, 2, 3\}$ for the neural network predictor used in the JAWA experiments (see Section 5.3), rounded up to the nearest second. This runtime experiment was performed on an 8-core personal computer with 32 GB of memory.

Method	Airfoil	Wine	Wave	Superconduct	Communities
JAW	58 min, 39 s	59 min, 18 s	1 hr, 24 min, 24 s	1 hr, 26 min, 53 s	1 hr, 25 min, 42 s
JAWA-1	1 s	2 s	4 s	7 s	8 s
JAWA-2	3 s	4 s	6 s	11 s	14 s
JAWA-3	11 s	12 s	16 s	21 s	23 s

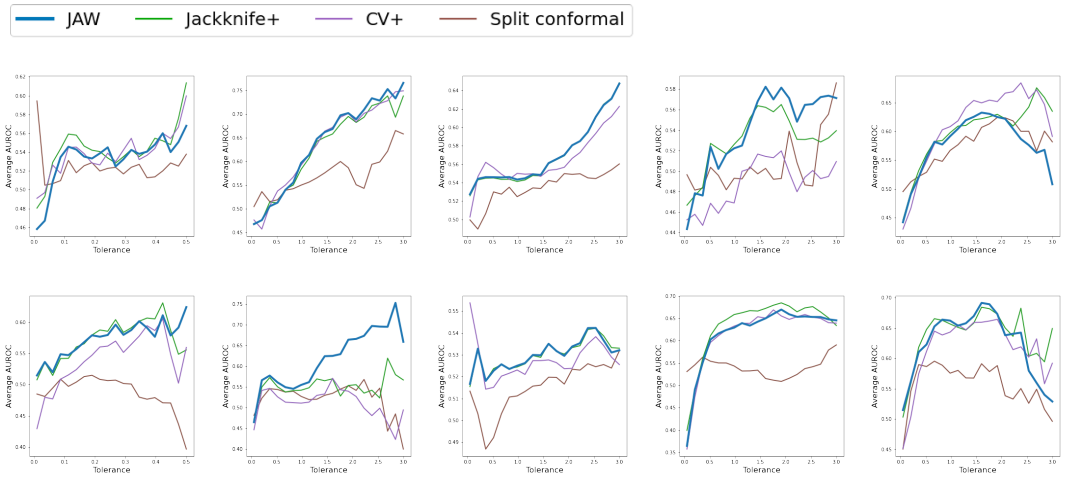

(a) Airfoil (b) Wine (c) Wave (d) Superconduct (e) Communities

Figure 8: AUROC values for different tolerance levels τ across the three datasets, and with neural network (top row) and random forest predictors (bottom row), averaged across 5 experiment replicates. JAW, jackknife+, and CV+ achieve comparably high AUROC values for most tolerance levels in most of the conditions, whereas split conformal has lower performance. JAW has noticeably higher AUROC values in the wine dataset for the random forest predictor.

5.4.4 Risk-assessment audit experiments for JAW and baselines: AUC

In this set of experiments, we turn to the risk-assessment audit task where the goal is to evaluate a method's ability to estimate the coverage of a given interval, or to estimate the risk that the true label lies outside some error threshold τ around the original prediction $\widehat{\mu}(X_{n+1})$. Given the prediction $\widehat{\mu}(X_{n+1})$ and an error threshold τ, define the interval of interest as $I(\widehat{\mu}(X_{n+1}), \tau) = [\widehat{\mu}(X_{n+1}) - \tau,\ \widehat{\mu}(X_{n+1}) + \tau]$. Then, the goal is to use each method's predictive distribution to estimate the probability that the prediction is correct or incorrect:

- $\widehat{\mu}(X_{n+1})$ is correct $\iff |Y_{n+1} - \widehat{\mu}(X_{n+1})| \leq \tau \iff Y_{n+1} \in I(\widehat{\mu}(X_{n+1}), \tau)$
- $\widehat{\mu}(X_{n+1})$ is incorrect $\iff |Y_{n+1} - \widehat{\mu}(X_{n+1})| > \tau \iff Y_{n+1} \notin I(\widehat{\mu}(X_{n+1}), \tau)$

We conduct these risk-assessment experiments on all five UCI datasets and for four predictive interval-generation methods that we repurpose to the risk assessment task (where "R" stands for the new task): JAW-R, jackknife+R, cross validation+R, and split conformal-R. Specifically, the jackknife+, CV+, and split methods (which all assume exchangeable data) are adapted to risk assessment using the approach proposed in Section 3.3, while JAW (which allows for covariate shift) is adapted to risk assessment using the approach proposed in Section 3.4. Five replicates of each experiment are conducted, and the results are estimated using area under the receiver operating characteristic curve (AUROC) for values of τ selected with uniform spacing in the interval $[q^{-}_{n,0.05}\{R_i^{LOO}\},\ q^{+}_{n,0.05}\{R_i^{LOO}\}]$ (between the 0.05 and 0.95 quantiles of the leave-one-out residual prediction errors) for a given dataset and $\widehat{\mu}$ function.

Figure 8 illustrates the ability for JAW and baseline methods' predictive distribution to detect errors in given intervals, that is in estimating the probability of the event $|Y_{n+1} - \widehat{\mu}(X_{n+1})| \leq \tau$ for a given tolerance τ. The y-axis for each plot is the mean area under the ROC curve across the experimental replicates, and the x-axis is the tolerance level τ. Better performing methods have higher overall AUROC values for all values τ. JAW achieves AUROC values comparable to jackknife+ and CV+ for most tolerance levels and across most $\widehat{\mu}$ and dataset conditions. In addition, JAW achieves higher AUROC values than all other methods in the wine dataset with the random forest predictor. These results seem to suggest that JAW may not offer a consistent benefit over the jackknife+ method in risk assessment, but that there may be a marginal benefit of JAW compared to jackknife+ for some datasets and conditions. We speculate that the seeming lack of substantial benefit of JAW over jackknife+ for the risk assessment may be due to the increased variance of the JAW predictive intervals under covariant shift due to the decrease in effective sample size discussed previously.

5.5 JAW-E: JAW with estimated weights

We also compare coverage histograms of JAW with oracle likelihood-ratio weights those of JAW-E with weights estimated from probabilstic classification. We follow the approach used in Tibshirani et al. [2019] for estimating the likelihood-ratio weights using logistic regression and random forest classifiers. Specifically, for training covariate data $X_1, ..., X_n$ and test covariate data $X_{n+1}, ..., X_{n+m}$ where $C_i = 0$ for $i = 1, ..., n$ and $C_i = 1$ for $i = n+1, ..., n+m$, the conditional odds ratio $\mathbb{P}(C = 1|X = x)/\mathbb{P}(C = 0|X = x)$ can be used as an equivalent substitute to the likelihood ratio weight function $w(x)$ due to the normalization of the weights for use in JAW. Thus, for an estimate $\widehat{p}(x) \approx \mathbb{P}(C = 1|X = x)$ obtained from a classifier such as logistic regression or random forest, then we can use the following estimated weight function in place of likelihood-ratio weights:

$$\widehat{w}(x) = \frac{\widehat{p}(x)}{1 - \widehat{p}(x)}. \tag{33}$$

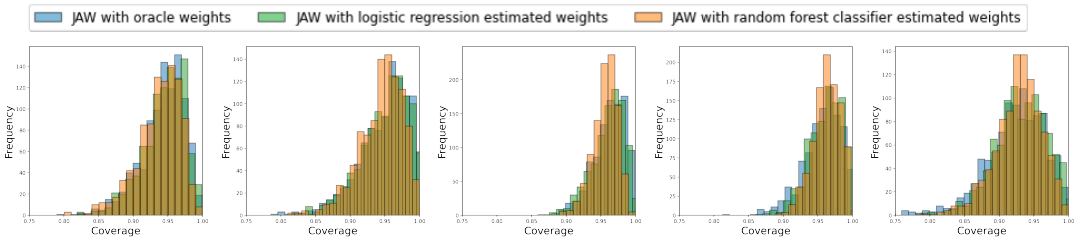

(a) Airfoil (b) Wine (c) Wave (d) Superconduct (e) Communities

Figure 9: Comparison of JAW coverage under covariate shift with oracle versus JAW-E coverage with estimated likelihood ratio weights for neural network predictor across all datasets. Blue is oracle weights, green is weights estimated with logistic regression, and orange is weights estimated with random forest classifier. Histograms represent 1000 experimental replicates.

Figure 9 illustrates the coverage performance of JAW-E, or JAW with estimated likelihood ratio weights, compared to JAW for weights estimated using both logistic regression and random forest classifiers as described in Section 5.3. Results are for both neural network and random forest regression predictors across all five UCI datasets. We observe that the coverage histograms for JAW-E with both weight estimation methods are largely directly overlapping with the coverage histogram for JAW with oracle weights. These results demonstrate the applicability of JAW-E for predictive inference under covariate shift when the true likelihood ratio is not known but can be estimated from the data.

5.6 Ablation studies on shift magnitudes

We demonstrate the effect of different magnitudes of covariate shift by comparing the coverage performance of JAW and the jackknife+ on the airfoil dataset with different magnitudes of the exponential tilting bias parameter β. Informed by these experiments depicted in Figure 10—where JAW's mean coverage remains consistent but the variance in coverage increases with increased covariate shift magnitude—we performed additional experiments to investigate the potential cause of JAW's increased variance. Specifically, we compare histograms of JAW's coverage at a fixed covariate shift magnitude to that of jackknife+ without covariate shift but with reduced "effective sample size", which is known to be reduced by likelihood ratio weighting. Tibshirani et al. [2019] made a similar comparison between weighted split conformal prediction under covariate shift and standard split conformal prediction with reduced effective sample size, and we use the same heuristic for effective sample size estimation [Gretton et al., 2009, Reddi et al., 2015] (which we also used for selecting exponential tilting parameter values for each dataset in Figure 6):

$$\widehat{n} = \frac{[\sum_{i=1}^{n} |w(X_i)|]^2}{\sum_{i=1}^{n} |w(X_i)|^2} = \frac{||w(X_{1:n})||_1^2}{||w(X_{1:n})||_2^2}.$$

Effect of different magnitudes of covariate shift As shown in Figure 10, the extent of covariate shift can be controlled by modifying a parameter in the exponential tilting weights so that weights are are more or less drastic. When the bias parameter is set to 0 this corresponds to no bias or IID train and test data. We can see that JAW is robust to different amounts of covariate shift, generating high coverage even under high level of shift.

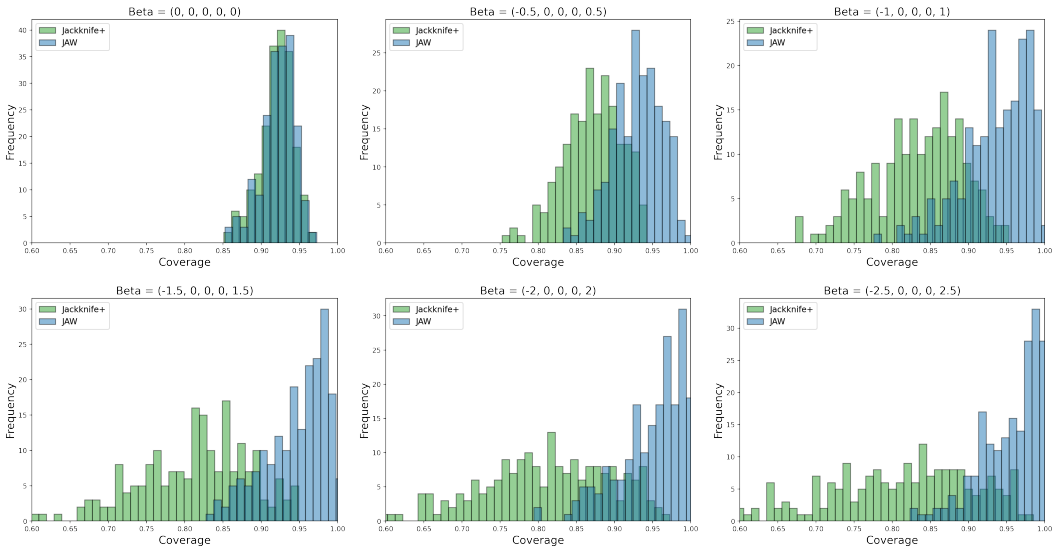

Figure 10: JAW performance compared to jackknife+ on the airfoil dataset with random forest $\widehat{\mu}$ function, under increasing magnitude of covariate shift (different β values), with 200 replicates.

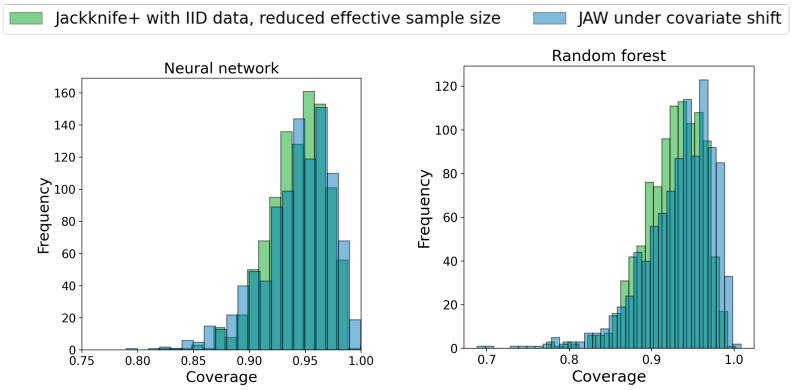

Figure 11: Comparison of JAW coverage histogram under covariate shift (blue) to jackknife+ coverage histogram (green) with no covariate shift but reduced effective sample size corresponding to the magnitude of covariate shift that JAW is evaluated on. Experiments are for both neural network (left) and random forest (right) predictors on the airfoil dataset, with 1000 experimental replicates. The largely overlapping histograms suggests that the increase in JAW coverage variance observed in Figure 10 is largely due to the decrease in effective sample size inherent to likelihood ratio weighting.

Reduced effective sample size accounts for JAW increase in coverage variance under shift While JAW's mean coverage remains relatively consistent under different magnitudes of covariate shift as seen in Figure 10, we also observe that the variance in coverage is higher for higher levels of shift. We hypothesized that this increase in variance is due to the high variance issue associated with important weighting methods that is well known [Reddi et al., 2015, Li et al., 2020] in the literature. We evaluate this hypothesis with effective sample size experiments reported in Figure 11 that compare a histogram of JAW's coverage under covariate shift with the coverage of jackknife+ with IID data but reduced effective sample size corresponding to the magnitude of covariate shift that

JAW is evaluated on (see Section 5.3 for details). In Figure 11 we see that the coverage histogram for JAW under covariate shift is nearly directly overlapping with the histogram for jackknife+ coverage with no shift but reduced effective sample size. This result suggests that the reduction of effective sample size due to likelihood ratio weighting is largely if not entirely responsible for the increase in JAW coverage variance for increased shift magnitudes. We leave the variance reduction of our work to the future work.

6 Conclusion and Future Work

In this paper, we study the problem of uncertainty quantification under covariate shift. We develop JAWS, a series of wrapper methods for distribution-free uncertainty quantification for when the data exchangeability assumption is violated due to covariate shift. We provide a rigorous coverage guarantee for our core predictive interval generation method JAW, the jackknife+ with likelihood-ratio weights, which relaxes the exchanageability assumption of the jackknife+ guarantee to allow for covariate shift. For computationally efficient estimation of JAW, we propose an approximation using higher-order influence functions called JAWA, which we demonstrate approaches the JAW coverage guarantee in the limit of the sample size or influence function order. We additionally propose a general framework for adapting any predictive interval generation method and associated coverage guarantee to the task of risk assessment, and present JAW-R and JAWA-R as the repurposed versions of our interval generation methods to risk assessment. We demonstrate superior empirical performance of our JAWS methods on a variety of datasets under covariate shift.

In practice, we do observe that JAW appears to have high variance in its coverage under covariate shift relative to the unweighted jackknife+ applied to exchangeable data. Additionally, we note that in extreme cases of covariate shift where the normalized likelihood ratio of the test point approaches or exceeds α, JAW and JAWA may produce overly large predictive intervals, though this is also a limitation of weighted conformal prediction [Tibshirani et al., 2019]. In the future, we are interesting in addressing the problems of reducing the variance in coverage and improving the sharpness of the predictive intervals.

Acknowledgments and Disclosure of Funding

This work was supported by the National Science Foundation grant IIS-1840088. We thank Yoav Wald for helpful discussions and advice, as well as Peter Schulam for sharing code that facilitated our influence function approximations and AUC experiments.

References

Scott Thiebes, Sebastian Lins, and Ali Sunyaev. Trustworthy artificial intelligence. *Electronic Markets*, 31(2):447–464, 2021.

Soumya Ghosh, Q Vera Liao, Karthikeyan Natesan Ramamurthy, Jiri Navratil, Prasanna Sattigeri, Kush R Varshney, and Yunfeng Zhang. Uncertainty quantification 360: A holistic toolkit for quantifying and communicating the uncertainty of ai. *arXiv preprint arXiv:2106.01410*, 2021.

Richard Tomsett, Alun Preece, Dave Braines, Federico Cerutti, Supriyo Chakraborty, Mani Srivastava, Gavin Pearson, and Lance Kaplan. Rapid trust calibration through interpretable and uncertainty-aware ai. *Patterns*, 1(4):100049, 2020.

Umang Bhatt, Javier Antorán, Yunfeng Zhang, Q Vera Liao, Prasanna Sattigeri, Riccardo Fogliato, Gabrielle Melançon, Ranganath Krishnan, Jason Stanley, Omesh Tickoo, et al. Uncertainty as a form of transparency: Measuring, communicating, and using uncertainty. In *Proceedings of the 2021 AAAI/ACM Conference on AI, Ethics, and Society*, pages 401–413, 2021.

Peter Schulam and Suchi Saria. Can you trust this prediction? auditing pointwise reliability after learning. In *The 22nd International Conference on Artificial Intelligence and Statistics*, pages 1022–1031. PMLR, 2019.

Yaniv Ovadia, Emily Fertig, Jie Ren, Zachary Nado, David Sculley, Sebastian Nowozin, Joshua Dillon, Balaji Lakshminarayanan, and Jasper Snoek. Can you trust your model's uncertainty?

evaluating predictive uncertainty under dataset shift. *Advances in neural information processing systems*, 32, 2019.

Dennis Ulmer, Lotta Meijerink, and Giovanni Cinà. Trust issues: Uncertainty estimation does not enable reliable ood detection on medical tabular data. In *Machine Learning for Health*, pages 341–354. PMLR, 2020.

Aurick Zhou and Sergey Levine. Amortized conditional normalized maximum likelihood: Reliable out of distribution uncertainty estimation. In *International Conference on Machine Learning*, pages 12803–12812. PMLR, 2021.

Alex Chan, Ahmed Alaa, Zhaozhi Qian, and Mihaela Van Der Schaar. Unlabelled data improves bayesian uncertainty calibration under covariate shift. In *International Conference on Machine Learning*, pages 1392–1402. PMLR, 2020.

Mary Feng, Gilmer Valdes, Nayha Dixit, and Timothy D Solberg. Machine learning in radiation oncology: opportunities, requirements, and needs. *Frontiers in oncology*, 8:110, 2018.

Elizabeth Huynh, Ahmed Hosny, Christian Guthier, Danielle S Bitterman, Steven F Petit, Daphne A Haas-Kogan, Benjamin Kann, Hugo JWL Aerts, and Raymond H Mak. Artificial intelligence in radiation oncology. *Nature Reviews Clinical Oncology*, 17(12):771–781, 2020.

Saul N Weingart, Lulu Zhang, Megan Sweeney, and Michael Hassett. Chemotherapy medication errors. *The Lancet Oncology*, 19(4):e191–e199, 2018.

Marcel Van Herk. Errors and margins in radiotherapy. In *Seminars in radiation oncology*, volume 14, pages 52–64. Elsevier, 2004.

Howard Gurney. How to calculate the dose of chemotherapy. *British journal of cancer*, 86(8): 1297–1302, 2002.

Michael R Cohen, Roger W Anderson, Richard M Attilio, Laurence Green, Raymond J Muller, and Jane M Pruemer. Preventing medication errors in cancer chemotherapy. *American Journal of Health-System Pharmacy*, 53(7):737–746, 1996.

Vladimir Vovk, Alexander Gammerman, and Glenn Shafer. *Algorithmic learning in a random world*. Springer Science & Business Media, 2005.

Glenn Shafer and Vladimir Vovk. A tutorial on conformal prediction. *Journal of Machine Learning Research*, 9(3), 2008.

Vladimir Vovk. Transductive conformal predictors. In *IFIP International Conference on Artificial Intelligence Applications and Innovations*, pages 348–360. Springer, 2013.

Rina Foygel Barber, Emmanuel J Candes, Aaditya Ramdas, and Ryan J Tibshirani. Predictive inference with the jackknife+. *The Annals of Statistics*, 49(1):486–507, 2021.

Ryan J Tibshirani, Rina Foygel Barber, Emmanuel Candes, and Aaditya Ramdas. Conformal prediction under covariate shift. *Advances in neural information processing systems*, 32, 2019.

Aleksandr Podkopaev and Aaditya Ramdas. Distribution-free uncertainty quantification for classification under label shift. In *Uncertainty in Artificial Intelligence*, pages 844–853. PMLR, 2021.

Dheeru Dua and Casey Graff. UCI machine learning repository, 2017. URL `http://archive.ics.uci.edu/ml`.

Masashi Sugiyama, Matthias Krauledat, and Klaus-Robert Müller. Covariate shift adaptation by importance weighted cross validation. *Journal of Machine Learning Research*, 8(5), 2007.

Hidetoshi Shimodaira. Improving predictive inference under covariate shift by weighting the log-likelihood function. *Journal of statistical planning and inference*, 90(2):227–244, 2000.

Gianluca Zeni, Matteo Fontana, and Simone Vantini. Conformal prediction: a unified review of theory and new challenges. *arXiv preprint arXiv:2005.07972*, 2020.

Eugene Ndiaye and Ichiro Takeuchi. Computing full conformal prediction set with approximate homotopy. *Advances in Neural Information Processing Systems*, 32, 2019.

Rina Foygel Barber, Emmanuel J Candes, Aaditya Ramdas, and Ryan J Tibshirani. Conformal prediction beyond exchangeability. *arXiv preprint arXiv:2202.13415*, 2022.

R Dennis Cook. Detection of influential observation in linear regression. *Technometrics*, 19(1):15–18, 1977.

Pang Wei Koh and Percy Liang. Understanding black-box predictions via influence functions. In *International conference on machine learning*, pages 1885–1894. PMLR, 2017.

Ryan Giordano, William Stephenson, Runjing Liu, Michael Jordan, and Tamara Broderick. A swiss army infinitesimal jackknife. In *The 22nd International Conference on Artificial Intelligence and Statistics*, pages 1139–1147. PMLR, 2019a.

Ryan Giordano, Michael I Jordan, and Tamara Broderick. A higher-order swiss army infinitesimal jackknife. *arXiv preprint arXiv:1907.12116*, 2019b.

Ahmed Alaa and Mihaela Van Der Schaar. Discriminative jackknife: Quantifying uncertainty in deep learning via higher-order influence functions. In *International Conference on Machine Learning*, pages 165–174. PMLR, 2020.

Steffen Bickel, Michael Brückner, and Tobias Scheffer. Discriminative learning under covariate shift. *Journal of Machine Learning Research*, 10(9), 2009.

Masashi Sugiyama, Taiji Suzuki, and Takafumi Kanamori. *Density ratio estimation in machine learning*. Cambridge University Press, 2012.

Arthur Gretton, Alex Smola, Jiayuan Huang, Marcel Schmittfull, Karsten Borgwardt, and Bernhard Schölkopf. Covariate shift by kernel mean matching. *Dataset shift in machine learning*, 3(4):5, 2009.

Yaoliang Yu and Csaba Szepesvári. Analysis of kernel mean matching under covariate shift. *arXiv preprint arXiv:1206.4650*, 2012.

Kai Zhang, Vincent Zheng, Qiaojun Wang, James Kwok, Qiang Yang, and Ivan Marsic. Covariate shift in hilbert space: A solution via sorrogate kernels. In *International Conference on Machine Learning*, pages 388–395. PMLR, 2013.

Yin Zhao, Longjun Cai, et al. Reducing the covariate shift by mirror samples in cross domain alignment. *Advances in Neural Information Processing Systems*, 34, 2021.

Anqi Liu and Brian Ziebart. Robust classification under sample selection bias. *Advances in neural information processing systems*, 27, 2014.

Xiangli Chen, Mathew Monfort, Anqi Liu, and Brian D Ziebart. Robust covariate shift regression. In *Artificial Intelligence and Statistics*, pages 1270–1279. PMLR, 2016.

John C Duchi, Tatsunori Hashimoto, and Hongseok Namkoong. Distributionally robust losses against mixture covariate shifts. *Under review*, 2, 2019.

Ashkan Rezaei, Anqi Liu, Omid Memarrast, and Brian D Ziebart. Robust fairness under covariate shift. In *Proceedings of the AAAI Conference on Artificial Intelligence*, volume 35, pages 9419–9427, 2021.

Vladimir Vovk, Ilia Nouretdinov, and Alex Gammerman. On-line predictive linear regression. *The Annals of Statistics*, pages 1566–1590, 2009.

Evgeny Burnaev and Vladimir Vovk. Efficiency of conformalized ridge regression. In *Conference on Learning Theory*, pages 605–622. PMLR, 2014.

Jing Lei and Larry Wasserman. Distribution-free prediction bands for non-parametric regression. *Journal of the Royal Statistical Society: Series B (Statistical Methodology)*, 76(1):71–96, 2014.

Jing Lei, Max G'Sell, Alessandro Rinaldo, Ryan J Tibshirani, and Larry Wasserman. Distribution-free predictive inference for regression. *Journal of the American Statistical Association*, 113(523): 1094–1111, 2018.

Harris Papadopoulos. *Inductive conformal prediction: Theory and application to neural networks*. INTECH Open Access Publisher Rijeka, 2008.

Vladimir Vovk. Conditional validity of inductive conformal predictors. In *Asian conference on machine learning*, pages 475–490. PMLR, 2012.

Ronald Butler and Edward D Rothman. Predictive intervals based on reuse of the sample. *Journal of the American Statistical Association*, 75(372):881–889, 1980.

Bradley Efron and Gail Gong. A leisurely look at the bootstrap, the jackknife, and cross-validation. *The American Statistician*, 37(1):36–48, 1983.

Seymour Geisser. The predictive sample reuse method with applications. *Journal of the American statistical Association*, 70(350):320–328, 1975.

Mervyn Stone. Cross-validatory choice and assessment of statistical predictions. *Journal of the royal statistical society: Series B (Methodological)*, 36(2):111–133, 1974.

Vladimir Vovk, Ilia Nouretdinov, Valery Manokhin, and Alexander Gammerman. Cross-conformal predictive distributions. In *Conformal and Probabilistic Prediction and Applications*, pages 37–51. PMLR, 2018.

Rupert G Miller. The jackknife-a review. *Biometrika*, 61(1):1–15, 1974.

Lukas Steinberger and Hannes Leeb. Conditional predictive inference for high-dimensional stable algorithms. *arXiv preprint arXiv:1809.01412*, 2018.

Lukas Steinberger and Hannes Leeb. Leave-one-out prediction intervals in linear regression models with many variables. *arXiv preprint arXiv:1602.05801*, 2016.

Luisa Turrin Fernholz. *Von Mises calculus for statistical functionals*, volume 19. Springer Science & Business Media, 2012.

Dougal Maclaurin, David Duvenaud, and Ryan P Adams. Autograd: Effortless gradients in numpy. In *ICML 2015 AutoML workshop*, volume 238, 2015.

Paulo Cortez, António Cerdeira, Fernando Almeida, Telmo Matos, and José Reis. Modeling wine preferences by data mining from physicochemical properties. *Decision support systems*, 47(4): 547–553, 2009.

Kam Hamidieh. A data-driven statistical model for predicting the critical temperature of a superconductor. *Computational Materials Science*, 154:346–354, 2018.

Michael Redmond and Alok Baveja. A data-driven software tool for enabling cooperative information sharing among police departments. *European Journal of Operational Research*, 141(3):660–678, 2002.

Sashank Reddi, Barnabas Poczos, and Alex Smola. Doubly robust covariate shift correction. In *Proceedings of the AAAI Conference on Artificial Intelligence*, volume 29, 2015.

Fengpei Li, Henry Lam, and Siddharth Prusty. Robust importance weighting for covariate shift. In *International Conference on Artificial Intelligence and Statistics*, pages 352–362. PMLR, 2020.

Anastasios Angelopoulos, Stephen Bates, Jitendra Malik, and Michael I Jordan. Uncertainty sets for image classifiers using conformal prediction. *arXiv preprint arXiv:2009.14193*, 2020.

A Proofs for theoretical results

A.1 Proof of Theorem 1

Proof. We use (a) - (d) to denote four setup steps, and we use 1-3 to denote the main steps in the proof. Our first two initial setup steps (a) and (b) are identical to the corresponding setup in the Barber et al. [2021] proof:

(a) First, we suppose the hypothetical case where in addition to the training data $\{(X_1, Y_1), ..., (X_n, Y_n)\}$, we also have access to the test point (X_{n+1}, Y_{n+1}). For each pair of indices $i, j \in \{1, ..., n+1\}$ with $i \neq j$, we define $\tilde{\mu}_{-(i,j)}$ as the regression function fitted on the training and test data except with the points i and j removed. (We follow the notation in Barber et al. [2021] where $\tilde{\mu}$ rather than $\widehat{\mu}$ reminds us that the former is fit on a subset of data $1, ..., n+1$ that may contain the test point $n+1$.) We note that $\tilde{\mu}_{-(i,j)} = \tilde{\mu}_{-(j,i)}$ for any $i \neq j$., and $\tilde{\mu}_{-(i,n+1)} = \widehat{\mu}_{-i}$ for any $i = 1, ..., n$.

(b) We also define the same matrix of residuals in Barber et al. [2021], $R \in \mathbb{R}^{(n+1)\times(n+1)}$, with entries

$$R_{ij} = \begin{cases} +\infty & i = j, \\ |Y_i - \tilde{\mu}_{-(i,j)}(X_i)| & i \neq j \end{cases}$$

such that the off-diagonal entries R_{ij} represent the residual for the ith datapoint where both i and j are not seen by the regression fitting.

At this point we begin to introduce some changes to the proof in Barber et al. [2021]:

(c) We define a weighted version of the comparison matrix in Barber et al. [2021], which we call $A^w \in \mathbb{R}^{(n+1)\times(n+1)}$, with entries $A^w_{ij} = w(X_i)w(X_j) \cdot \mathbb{1}\{R_{ij} > R_{ji}\}$

That is, $\mathbb{1}\{R_{ij} > R_{ji}\}$ is the indicator for the event that, when i and j are excluded from the regression fitting, i has larger residual than j; A^w_{ij} is this indicator multiplied by $w(X_i)w(X_j)$, the product of the likelihood ratios for points i and j. For any $i, j = 1, ..., n+1$, note that $A^w_{ij} > 0$ implies $A^w_{ji} = 0$ for any $i, j = 1, ..., n+1$. Moreover, note that in the absence of covariate shift, $w(X_i) = w(X_j) = 1$ for all $i, j = 1, ..., n+1$ and the weighted comparison matrix A^w is equivalent to the unweighted comparison matrix A described in Barber et al. [2021].

(d) Next, as in Barber et al. [2021] we are interested in identifying points that have unusually large residuals and are thus hard to predict. Barber et al. [2021] defined such points with unusually large residuals as points i where $\mathbb{1}\{R_{ij} > R_{ji}\}$ for a sufficiently large fraction of other points j. However, in the covariate shift setting, we need to account for the fact that the informativeness of the comparison $\mathbb{1}\{R_{ij} > R_{ji}\}$ depends on the likelihood ratio of j; if $w(X_j) > w(X_{j'})$ for some points $j, j' \in \{1, ..., n+1\}\backslash i,\ j \neq j'$, then the comparison $\mathbb{1}\{R_{ij} > R_{ji}\}$ should contain more information about how difficult i is to predict than the comparison $\mathbb{1}\{R_{ij'} > R_{j'i}\}$. In particular, we are interested in identifying points i where $\mathbb{1}\{R_{ij} > R_{ji}\}$ for a sufficiently large *total normalized weight* of other points j. With this motivation, we define the set of "strange" points $\mathcal{S}(A^w) \subseteq \{1, ..., n+1\}$ in the following two equivalent ways that each serve a different illustrative purpose:

$$\mathcal{S}(A^w) = \left\{ i \in \{1, ..., n+1\} \ :\ w(X_i) > 0, \quad \sum_{j=1}^{n+1} \left(p^w_j(X_{1:(n+1)}) \cdot \mathbb{1}\{R_{ij} > R_{ji}\} \right) \geq 1 - \alpha \right\}$$

$$= \left\{ i \in \{1, ..., n+1\} \ :\ w(X_i) > 0, \quad \frac{\sum_{j=1}^{n+1} A^w_{ij}}{w(X_i) \sum_{k=1}^{n+1} w(X_k)} \geq 1 - \alpha \right\}$$

The first definition is the best representation for our intuition of $\mathcal{S}(A^w)$ as a set of "strange" points, which we have described. That is, in the first definition it is straightforward to see how $\mathcal{S}(A^w) \subseteq \{1, ..., n+1\}$ is the set of points $i \in \{1, ..., n+1\}$ such that for all the points $j \in \{1, ..., n+1\}, j \neq i$ where $R_{ij} > R_{ji}$, that the sum of the normalized weights $p^w_j(X_{1:(n+1)})$ of all such points j is sufficiently large (at least $1 - \alpha$). On the other hand, the second definition represents how the set of strange points can be computed from the

weighted comparison matrix A^w and the likelihood ratio weights w. Note that in the second definition, when $w(X_k) = 1$ for all $k = 1, ..., n+1$ it is straightforward to see that $\mathcal{S}(A^w)$ is equivalent to the set of strange points $\mathcal{S}(A)$ in the Barber et al. [2021] proof (to see this, observe that in this case $\sum_{k=1}^{n+1} w(X_k) = n + 1$).

The following main steps in our proof take the following structure, similar to as in Barber et al. [2021]:

- Step 1: Establish deterministically that $\sum_{i \in \mathcal{S}(A^w)} p_i^w(x) \leq 2\alpha$. That is, for any comparison matrix A^w, it is impossible to have the total normalized weight of all the strange points exceed 2α.
- Step 2: Using the fact that the datapoints are weighted exchangeable, show that the probability that the test point $n + 1$ is strange (i.e., $n + 1 \in \mathcal{S}(A^w)$) is thus bounded by 2α.
- Step 3: Lastly, verify that the JAW interval can only fail to cover the test label value Y_{n+1} if $n + 1$ is a strange point.

Step 1: Bounding the total normalized weight of the strange points. This proof step follows and generalizes the corresponding proof step in Barber et al. [2021] that relies on Landau's theorem for tournaments. For each pair of points i and j where $i \neq j$, let us say that i "wins" its game against point j if $A_{ij}^w > 0$, that is if both i and j have nonzero density in the test distribution and if there is a higher residual on point i than on point j for the regression model $\tilde{\mu}_{-(i,j)}$. We say that i loses its game with j otherwise.

However, whereas Barber et al. [2021] derive a bound on the *number* of strange points from a bound on the *number of pairs* of strange points, we instead derive a bound on the *total normalized weight* of the strange points from a bound on the sum of the *product of normalized weights* for two strange points in a pair. As we will see, this idea generalizes the idea of counting pairs of points to account for continuous weights on the points: If all points have uniform unnormalized weight of 1, then, after adjusting for a normalizing constant in our construction, the product of unnormalized weights of points in a pair is 1 for all pairs and our construction reduces to bounding the number of distinct pairs of strange points.

Observe that, by the definition of a strange point, the points that each strange point $i \in \mathcal{S}(A^w)$ wins against must have total normalized weight greater than or equal to $(1 - \alpha)$, and thus the points that each strange point $i \in \mathcal{S}(A^w)$ loses to can only have total normalized weight at most $\alpha - p_i^w(X_{1:(n+1)})$ (our definition does not allow i to lose to itself). That is:

$$\text{Total normalized weight of points that } i \text{ loses to} = \sum_{j=1}^{n+1} \left(p_j^w(X_{1:(n+1)}) \cdot \mathbb{1}\{R_{ij} \leq R_{ji}\} \right) \leq \alpha - p_i^w(X_{1:(n+1)})$$

This inequality will help us obtain an upper bound on the sum of the product of normalized weights between strange points in a pair. To aid with intuition, it may be helpful to think about a correspondance between a product of two weights and the area of a rectangle with side lengths equal to each weight value. Suppose that for each strange point $i \in \mathcal{S}(A^w)$ we construct a rectangle L_i with width equal point i's normalized weight, $p_i^w(X_{1:(n+1)})$, and length equal to the largest total normalized weight that the points that i loses to could have, $\alpha - p_i^w(X_{1:(n+1)})$ (i cannot lose to itself). In addition, suppose that we also construct a second rectangle L_i' for each strange point $i \in \mathcal{S}(A^w)$ with width equal to $p_i^w(X_{1:(n+1)})$—note that L_i' has the same width as L_i—but with length equal to half the total normalized weight of all of the strange points other than i, that is, $\frac{1}{2} \sum_{j \in \mathcal{S}(A^w) \setminus i} p_j^w(X_{1:(n+1)})$.

Observe that the total area of the set of rectangles $\{L_i\}$ is an upper bound on the sum of products of normalized weights for all points in a pair where one point is a strange point and the other point is a point that the strange point loses to. To see this, note that the length of each L_i can be partitioned based on the normalized weights of the points that i loses to so that, for each point j that i loses to, there is a rectangle contained in L_i—call it L_{ij}—with width $p_i^w(X_{1:(n+1)})$ and length $p_j^w(X_{1:(n+1)})$, where for $j \neq j'$, L_{ij} and $L_{ij'}$ overlap at most at their boundary. Thus the area of L_i is at least the total area of these smaller rectangles $\{L_{ij}\}$ that are contained within L_i, that is $\sum_{j: i \text{ loses to } j} \text{Area}(L_{ij}) \leq \text{Area}(L_i)$, and therefore the total area of $\{L_i\}$ is as described.

On the other hand, the total area of the set of rectangles $\{L'_i\}$ is the sum of the product of the normalized weights of two strange points in a pair over all pairs of strange points, where the factor of $\frac{1}{2}$ avoids double counting the pairs of strange points. To see this, note that for every pair of strange points $\{i, j\}$ there is a distinct subrectangle—call it L'_{ij}—that is contained in L'_i, such that L'_{ij} has width $p_i^w(X_{1:(n+1)})$ and length $\frac{1}{2}p_j^w(X_{1:(n+1)})$, where for $j \neq j'$, L_{ij} and $L_{ij'}$ overlap at most at their boundary. Moreover, for every pair of strange points $\{i, j\}$ there is also an analogous subrectangle L'_{ji} with width $p_j^w(X_{1:(n+1)})$ and length $\frac{1}{2}p_i^w(X_{1:(n+1)})$. Thus, the combined area of L'_{ji} and L'_{ij} is $\text{Area}(L'_{ij}) + \text{Area}(L'_{ji}) = p_i^w(X_{1:(n+1)}) \cdot p_j^w(X_{1:(n+1)})$, and the total area of $\{L'_i\}$ is as described. (Furthermore, note that when the unnormalized weights are all equal to 1, the area of $\{L'_i\}$, adjusted by a normalization constant, is equivalent to the total number of pairs of strange points $s(s-1)/2$, where $s = |S(A^w)|$ is the number of strange points.)

Now, observe that every pair of two strange points is also a pair of points where one point is strange and the other is a point that the strange point loses to, so the set of pairs of points included in the construction of $\{L'_i\}$ is a subset of the set of pairs of points for which the area of $\{L_i\}$ is the upper bound previously described. To be more precise, let $\{i, j\}$ be a pair of strange points, where WLOG let us say i loses to j. Then, for the L'_{ij} and L'_{ji} contained within $\{L'_i\}$ as described before, there exists a distinct L_{ij} contained within $\{L_i\}$, such that $\text{Area}(L'_{ij}) + \text{Area}(L'_{ji}) = \text{Area}(L_{ij})$. More generally, we see that the total area of all the subrectangles $\{L'_{ij}\}$ is bounded by the total area of the subrectangles $\{L_{ij}\}$, that is $\sum_{i,j \in \mathcal{S}(A^w),\ i \neq j} \text{Area}(L'_{ij}) = \sum_{i,j \in \mathcal{S}(A^w),\ i \neq j} \text{Area}(L_{ij}) \leq \sum_{i \in \mathcal{S}(A^w),\ i \text{ loses to } j} \text{Area}(L_{ij})$. Moreover, by construction $\sum_{i,j \in \mathcal{S}(A^w),\ i \neq j} \text{Area}(L'_{ij}) = \sum_{i \in \mathcal{S}(A^w)} \text{Area}(L'_i)$ and $\sum_{i \in \mathcal{S}(A^w),\ i \text{ loses to } j} \text{Area}(L_{ij}) \leq \sum_{i \in \mathcal{S}(A^w)} \text{Area}(L_i)$. Therefore, the area of the set of rectangles $\{L'_i\}$ is less than or equal to the area of rectangles $\{L_i\}$, which we can write as follows:

$$\sum_{i \in \mathcal{S}(A^w)} \text{Area}(L'_i) \leq \sum_{i \in \mathcal{S}(A^w)} \text{Area}(L_i)$$

$$\sum_{i \in \mathcal{S}(A^w)} \Big(p_i^w(X_{1:(n+1)}) \cdot \frac{1}{2} \sum_{j \in \mathcal{S}(A^w) \setminus i} p_j^w(X_{1:(n+1)}) \Big) \leq \sum_{i \in \mathcal{S}(A^w)} \Big(p_i^w(X_{1:(n+1)}) \cdot \big(\alpha - p_i^w(X_{1:(n+1)})\big) \Big)$$

Recall that we defined $p_i^w(X_{1:(n+1)}) = w(X_i) / \sum_{k=1}^{n+1} w(X_k)\ \forall\, i \in \{1, ..., n+1\}$, so in the uniform weighted case where $w(X_i) = 1\ \forall\, i \in \{1, ..., n+1\}$ then $\sum_{k=1}^{n+1} w(X_k) = n+1$, and multiplying both sides of the inequality above by $(n+1)^2$ yields the analogous inequality in Barber et al. [2021] that bounds the number of pairs of points.

We now proceed to solve for an upper bound on $\sum_{i \in \mathcal{S}(A^w)} p_i^w(X_{1:(n+1)})$:

$$\frac{1}{2} \sum_{i \in \mathcal{S}(A^w)} \Big(p_i^w(X_{1:(n+1)}) \cdot \sum_{j \in \mathcal{S}(A^w) \setminus i} p_j^w(X_{1:(n+1)}) \Big) \leq \sum_{i \in \mathcal{S}(A^w)} \Big(p_i^w(X_{1:(n+1)}) \cdot \big(\alpha - p_i^w(X_{1:(n+1)})\big) \Big)$$

$$\frac{1}{2} \sum_{i,j \in \mathcal{S}(A^w),\ i \neq j} p_i^w(X_{1:(n+1)}) p_j^w(X_{1:(n+1)}) \leq \quad \alpha \sum_{i \in \mathcal{S}(A^w)} p_i^w(X_{1:(n+1)}) \ - \sum_{i \in \mathcal{S}(A^w)} p_i^w(X_{1:(n+1)})^2$$

$$\frac{1}{2} \Bigg(\sum_{i \in \mathcal{S}(A^w)} p_i^w(X_{1:(n+1)})^2 \ + \sum_{i,j \in \mathcal{S}(A^w)} p_i^w(X_{1:(n+1)}) p_j^w(X_{1:(n+1)}) \Bigg) \leq \quad \alpha \sum_{i \in \mathcal{S}(A^w)} p_i^w(X_{1:(n+1)})$$

$$\frac{1}{2} \Bigg(\sum_{i \in \mathcal{S}(A^w)} p_i^w(X_{1:(n+1)})^2 \ + \sum_{i \in \mathcal{S}(A^w)} \Big(p_i^w(X_{1:(n+1)}) \cdot \sum_{j \in \mathcal{S}(A^w)} p_j^w(X_{1:(n+1)}) \Big) \Bigg) \leq \quad \alpha \sum_{i \in \mathcal{S}(A^w)} p_i^w(X_{1:(n+1)})$$

$$\frac{1}{2} \Bigg(\sum_{i \in \mathcal{S}(A^w)} p_i^w(X_{1:(n+1)})^2 \ + \Big(\sum_{i \in \mathcal{S}(A^w)} p_i^w(X_{1:(n+1)}) \Big)^2 \Bigg) \leq \quad \alpha \sum_{i \in \mathcal{S}(A^w)} p_i^w(X_{1:(n+1)})$$

$$\frac{\sum_{i \in \mathcal{S}(A^w)} p_i^w(X_{1:(n+1)})^2}{\sum_{i \in \mathcal{S}(A^w)} p_i^w(X_{1:(n+1)})} \ + \Big(\sum_{i \in \mathcal{S}(A^w)} p_i^w(X_{1:(n+1)}) \Big) \leq 2\alpha$$

$$\sum_{i \in \mathcal{S}(A^w)} p_i^w(X_{1:(n+1)}) \leq 2\alpha - \frac{\sum_{i \in \mathcal{S}(A^w)} p_i^w(X_{1:(n+1)})^2}{\sum_{i \in \mathcal{S}(A^w)} p_i^w(X_{1:(n+1)})}$$

where because $0 \leq p_i^w(X_{1:(n+1)}) \leq 1 \; \forall \; i = 1, ..., n+1$ and $p_i^w(X_{1:(n+1)}) > 0$ for some $i \in \{1, ..., n+1\}$, we have $0 \leq p_i^w(X_{1:(n+1)})^2 \leq p_i^w(X_{1:(n+1)}) \; \forall \; i = 1, ..., n+1$ and thus $0 \leq \frac{\sum_{i \in \mathcal{S}(A^w)} p_i^w(X_{1:(n+1)})^2}{\sum_{i \in \mathcal{S}(A^w)} p_i^w(X_{1:(n+1)})} \leq 1$, and we have

$$\sum_{i \in \mathcal{S}(A^w)} p_i^w(X_{1:(n+1)}) \leq 2\alpha \tag{34}$$

as desired.

Step 2: Weighted exchangeability of the datapoints. We now leverage the weighted exchangeability of the data to show that, since the total weight of the strange points is at most 2α, that a test point has at most 2α probability of being strange.

Note that the datapoints $(X_1, Y_1), ..., (X_{n+1}, Y_{n+1})$ are weighted exchangeable with a regression fitting algorithm $\mathcal{A}$ that is invariant to the ordering of the data. As a result, $\mathbb{1}\{R_{ij} > R_{ji}\}$ are weighted exchangeable random variables such that $w(X_i)w(X_j)\mathbb{1}\{R_{ij} > R_{ji}\}$ can be treated exchangeably, and thus it follows that $A^w \overset{\text{d}}{=} \Pi A^w \Pi^T$ for any $(n+1) \times (n+1)$ permutation matrix Π, where $\overset{\text{d}}{=}$ denotes equality in disribution.

Specifically, for any index $j \in \{1, ..., n+1\}$, suppose take Π to be the permutation matrix with $\Pi_{j,n+1} = 1$ (a permutation mapping $n+1$ to j). Then, deterministically

$$n+1 \in \mathcal{S}(A^w) \iff j \in \mathcal{S}(\Pi A^w \Pi^T)$$

so thus

$$\mathbb{P}\{n+1 \in \mathcal{S}(A^w)\} = \mathbb{P}\{j \in \mathcal{S}(\Pi A^w \Pi^T)\} = \mathbb{P}\{j \in \mathcal{S}(A^w)\}$$

for all $j = 1, ..., n+1$. That is, an arbitrary training point j is equally likely to be strange as the test point $n+1$. So, $\mathbb{P}\{n+1 \in \mathcal{S}(A^w)\}$ can be expressed as a weighted average of the $\mathbb{P}\{j \in \mathcal{S}(A^w)\}$ (though $\mathbb{P}\{n+1 \in \mathcal{S}(A^w)\} = \mathbb{P}\{j \in \mathcal{S}(A^w)\}$, we can take a weighted average to account for different likelihoods of point j in the test distribution relative to training):

$$\begin{aligned}
\mathbb{P}\{n+1 \in \mathcal{S}(A^w)\} &= \frac{1}{\sum_{k=1}^{n+1} w(X_k)} \sum_{j=1}^{n+1} w(X_j) \cdot \mathbb{P}\{j \in \mathcal{S}(A^w)\} \\
&= \sum_{j=1}^{n+1} p_j^w(X_{1:(n+1)}) \cdot \mathbb{P}\{j \in \mathcal{S}(A^w)\} \\
&= \mathbb{E}\left[\sum_{j \in \mathcal{S}(A^W)} p_j^w(X_{1:(n+1)})\right] \\
&\leq 2\alpha
\end{aligned}$$

Step 3: Connection to JAW: We would now like to connect our strange point result from step 2 to coverage of the JAW prediction interval. Following the approach of Barber et al. [2021], suppose that $Y_{n+1} \notin \widehat{C}^{\text{JAW}}_{n,\alpha}(X_{n+1})$. Then, either

$$\begin{aligned}
Y_{n+1} &> \widehat{q}^{+}_{n,\alpha}\{p_i^w(X_{1:(n+1)})\delta_{\widehat{\mu}_{-i}(X_{n+1})+R_i^{LOO}}\} \\
&\implies \sum_{i=1}^{n} p_i^w(X_{1:(n+1)}) \cdot \mathbb{1}\{Y_{n+1} > \widehat{\mu}_{-i}(X_{n+1}) + R_i^{LOO}\} \geq 1-\alpha
\end{aligned}$$

or otherwise

$$\begin{aligned}
Y_{n+1} &< \widehat{q}^{-}_{n,\alpha}\{p_i^w(X_{1:(n+1)})\delta_{\widehat{\mu}_{-i}(X_{n+1})+R_i^{LOO}}\} \\
&\implies \sum_{i=1}^{n} p_i^w(X_{1:(n+1)}) \cdot \mathbb{1}\{Y_{n+1} < \widehat{\mu}_{-i}(X_{n+1}) - R_i^{LOO}\} \geq 1-\alpha
\end{aligned}$$

And we can write the union of these two events as

$$\begin{aligned}
1-\alpha &\leq \sum_{i=1}^{n} p_i^w(X_{1:(n+1)}) \cdot \mathbb{1}\{Y_{n+1} \notin \widehat{\mu}_{-i}(X_{n+1}) \pm R_i^{LOO}\} \\
&= \sum_{i=1}^{n} p_i^w(X_{1:(n+1)}) \cdot \mathbb{1}\{|Y_j - \widehat{\mu}_{-j}(X_j)| < |Y_{n+1} - \widehat{\mu}_{-j}(X_{n+1})|\} \\
&= \sum_{i=1}^{n+1} p_i^w(X_{1:(n+1)}) \cdot \mathbb{1}\{R_{j,n+1} < R_{n+1,j}\}
\end{aligned}$$

from which we see that $n+1 \in \mathcal{S}(A^w)$—that is, $n+1$ is a strange point. This result together with the result from Step 2 gives us

$$\begin{aligned}
&\mathbb{P}\{Y_{n+1} \notin \widehat{C}_{n,\alpha}^{\text{JAW}}(X_{n+1})\} \leq \mathbb{P}\{n+1 \in \mathcal{S}(A^w)\} \leq 2\alpha \\
\therefore\ &\mathbb{P}\{Y_{n+1} \in \widehat{C}_{n,\alpha}^{\text{JAW}}(X_{n+1})\} \geq 1-2\alpha
\end{aligned}$$

□

A.2 Proof of Theorem 2

Proof. First, assume that Assumptions 1 - 4 and Condition 2 from Giordano et al. [2019b] hold uniformly for all n (where n is the number of training points). Then, Proposition 1 from Giordano et al. [2019b] establishes that

$$\max_{i\in[n]} \left|\left|\hat{\theta}_{-i}^{\text{IF-}K} - \hat{\theta}_{-i}\right|\right|_2 = O_p(N^{-\frac{1}{2}(K+1)}) \tag{35}$$

So, for fixed K:

$$\lim_{N\to\infty} \max_{i\in[n]} \left|\left|\hat{\theta}_{-i}^{\text{IF-}K} - \hat{\theta}_{-i}\right|\right|_2 = O_p(N^{-\frac{1}{2}(K+1)}) = 0 \tag{36}$$

Or, for fixed N:

$$\lim_{K\to\infty} \max_{i\in[n]} \left|\left|\hat{\theta}_{-i}^{\text{IF-}K} - \hat{\theta}_{-i}\right|\right|_2 = O_p(N^{-\frac{1}{2}(K+1)}) = 0 \tag{37}$$

Thus, $\hat{\theta}_{-i}^{\text{IF-}K} \to \hat{\theta}_{-i}$ as either $N \to \infty$ or $K \to \infty$. This implies that $\widehat{\mu}_{-i}^{\text{IF-}K} \to \widehat{\mu}_{-i}$ as either $N \to \infty$ or $K \to \infty$ because the model $\widehat{\mu}_{-i}$ is fully determined by its parameters $\hat{\theta}_{-i}$. Therefore, $\widehat{C}_{n,\alpha}^{\text{JAWA-}K}(X_{n+1}) \to \widehat{C}_{n,\alpha}^{\text{JAW}}(X_{n+1})$ in the limit of N or K, and thus by Theorem 1, $\mathbb{P}\{Y_{n+1} \in \widehat{C}_{n,\alpha}^{\text{JAWA-}K}(X_{n+1})\} \geq 1-2\alpha$ as $N \to \infty$ or $K \to \infty$.

Now, separately assume that Assumptions 1 - 4 and Condition 4 from Giordano et al. [2019b] hold uniformly for all n. Then, Proposition 3 from Giordano et al. [2019b] gives that

$$\max_{i\in[n]} \left|\left|\hat{\theta}_{-i}^{\text{IF-}K} - \hat{\theta}_{-i}\right|\right|_2 = O(N^{-(K+1)}) \tag{38}$$

The rest follows from a similar argument as when we assumed Condition 2. □

A.3 Proof of Theorem 3

Proof. Note that by construction $\widehat{C}_{n,\alpha_I}^{\text{audit}}(X_{n+1}) \subseteq I$, which implies $\mathbb{P}\{Y_{n+1} \in I\} \geq \mathbb{P}\{Y_{n+1} \in \widehat{C}_{n,\alpha_I}^{\text{audit}}(X_{n+1})\}$. If $\left\{\alpha' : a_L \leq q_{n,\alpha'}^{-}\{\frac{1}{n+1}\delta_{V_i^L}\},\ q_{n,\alpha'}^{+}\{\frac{1}{n+1}\delta_{V_i^U}\} \leq a_U\right\} \neq \emptyset$ and $\alpha_I < \frac{1-c_2}{c_1}$, then by the coverage guarantee for $\widehat{C}_{n,\alpha_I}^{\text{audit}}(X_{n+1})$ it follows that

$$\mathbb{P}\{Y_{n+1} \in I\} \geq \mathbb{P}\{Y_{n+1} \in \widehat{C}^{\text{audit}}_{n,\alpha_I}(X_{n+1})\} \geq 1 - c_1\alpha_I^{\text{audit}} - c_2 \tag{39}$$

Otherwise, either $\left\{\alpha' \ : \ a_L \leq \ q^-_{n,\alpha'}\{\frac{1}{n+1}\delta_{V_i^L}\} \ , \ q^+_{n,\alpha'}\{\frac{1}{n+1}\delta_{V_i^U}\} \leq a_U\right\} = \emptyset$ or we have $\alpha_I^{\text{audit}} \geq \frac{1-c_2}{c_1} \implies 1 - c_1\alpha_I^{\text{audit}} - c_2 \leq 0$. We cannot give a nontrivial (positive) coverage guarantee for I in either of these cases, so for these cases

$$\mathbb{P}\{Y_{n+1} \in I\} \geq \mathbb{P}\{Y_{n+1} \in \widehat{C}^{\text{audit}}_{n,\alpha_I}(X_{n+1})\} \geq 0 \tag{40}$$

□

A.4 Proof of Theorem 4

Proof. The proof is similar to the proof for Theorem 2, except with normalized likelihood ratio weights to account for covariate shift. Note that by construction $\widehat{C}^{\text{audit}}_{n,\alpha_I}(X_{n+1}) \subseteq I$, which implies $\mathbb{P}\{Y_{n+1} \in I\} \geq \mathbb{P}\{Y_{n+1} \in \widehat{C}^{\text{audit}}_{n,\alpha_I}(X_{n+1})\}$. If $\left\{\alpha' \ : \ a_L \leq q^-_{n,\alpha'}\{p_i^w(x)\delta_{V_i^L}\} \ , \ q^+_{n,\alpha'}\{p_i^w(x)\delta_{V_i^U}\} \leq a_U\right\} \neq \emptyset$ and $\alpha_I < \frac{1-c_2}{c_1}$, then by the coverage guarantee for $\widehat{C}^{\text{w-audit}}_{n,\alpha_I}(X_{n+1})$ it follows that

$$\mathbb{P}\{Y_{n+1} \in I\} \geq \mathbb{P}\{Y_{n+1} \in \widehat{C}^{\text{w-audit}}_{n,\alpha_I}(X_{n+1})\} \geq 1 - c_1\alpha_I^{\text{w-audit}} - c_2 \tag{41}$$

Otherwise, either $\left\{\alpha' \ : \ a_L \leq \ q^-_{n,\alpha'}\{p_i^w(x)\delta_{V_i^L}\} \ , \ q^+_{n,\alpha'}\{p_i^w(x)\delta_{V_i^U}\} \leq a_U\right\} = \emptyset$ or we have $\alpha_I^{\text{w-audit}} \geq \frac{1-c_2}{c_1} \implies 1 - c_1\alpha_I^{\text{w-audit}} - c_2 \leq 0$. We cannot give a nontrivial (positive) coverage guarantee for I in either of these cases, so for these cases

$$\mathbb{P}\{Y_{n+1} \in I\} \geq \mathbb{P}\{Y_{n+1} \in \widehat{C}^{\text{w-audit}}_{n,\alpha_I}(X_{n+1})\} \geq 0 \tag{42}$$

□

B Additional experimental details and analysis

B.1 Creation of covariate shift

That is, for a training set size of 200 points for each dataset, the exponential tilting parameters were selected and tuned so that the estimated effective sample size of the training data was reduced to approximately 50, averaged across 1000 random train-test splits. For training data $X_1, ..., X_n$ and likelihood ratio w, the effective sample size was estimated using the following commonly-used heuristic $\widehat{n} = [\sum_{i=1}^{n} |w(X_i)|]^2 / \sum_{i=1}^{n} |w(X_i)|^2$ [Gretton et al., 2009, Reddi et al., 2015, Tibshirani et al., 2019].

The specific selections of β that resulted in approximately $\widehat{n} = 50$ for each dataset are as follows. For the airfoil dataset, unless otherwise specified the tilting parameter was $\beta_{\text{airfoil}} = (-0.85, 0, 0, 0, 0.85)$, which induced covariate shift such that points with low values of the first feature and high values of the last feature were more likely to appear in the test distribution (see Figure 5). The wine dataset was similarly tilted using the first and last components, with a tilting parameter of $\beta_{\text{wine}} = (-0.53, 0, ..., 0, 0.53)$. The wave dataset is composed of 48 total features, of which the first 32 features are latitude and longitude values, and where the remaining 16 features are absorbed power values. Accordingly, the first principal component of only the 32 location features was used for tilting along with the first principal component of only the 16 absorbed power values, with a tilting parameter of $\beta_{\text{wave}} = (-0.0000925, 0.0000925)$ unless otherwise specified. For the superconductivity dataset, only the first principal component of all of the data was used for tilting, with tilting parameter $\beta_{\text{superconduct}} = 0.00062$. Lastly, for the communities and crime dataset, the first two principal components of the whole dataset were used with tilting parameter $\beta_{\text{communities}} = (-0.825, 0.825)$.

B.2 L2 regularization for IF experiments

The grid search evaluated the coverage of the first-order influence function approximation of the jackknife+ at different values of the regularization tuning parameter $\lambda \in \{0.5, 1, 2, 4, 8, 16, 32, 64, 96, 128\}$ for 10 train-test splits among all data for a dataset aside from the holdout tuning set. The smallest value of λ in the grid search for which the coverage of the first-order influence function approximation of the jackknife+ exceeded 0.875 was used. The coverage calibration threshold of 0.875 was selected because the change in coverage due to increased λ appeared to plateau just above or below the target coverage rate of 0.9 for each dataset, so setting the threshold slightly below 0.9 can help avoid over-regularizing. See Angelopoulos et al. [2020] for a discussion of calibrating uncertainty estimation in conformal prediction. This grid search procedure identified a separate λ regularization parameter for each dataset: $\lambda_{\text{air}} = 1, \lambda_{\text{win}} = 8, \lambda_{\text{wav}} = 4, \lambda_{\text{sup}} = 96, \lambda_{\text{com}} = 64$.

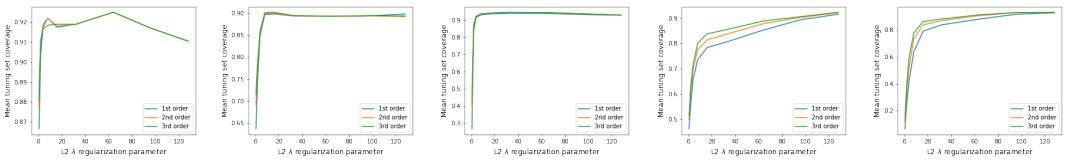

(a) Airfoil (b) Wine (c) Wave (d) Superconduct (e) Communities

Figure 12: Grid search plots for tuning the λ L2 regularization parameter for influence function coverage experiments. All experiments are done with 1st, 2nd, and 3rd order influence function approximations of the jackkinfe+ (denoted in blue, orange, and green lines in the figure). The y-axis for each plot is the average coverage on the tuning dataset for each L2 regularization parameter $\lambda \in \{0.5, 1, 2, 4, 8, 16, 32, 64, 96, 128\}$.

Cases where jackknife+ may not lose coverage Although JAW maintains significantly higher coverage than jackknife+ in most conditions, our results suggest that there are some cases when jackknife+ may not lose coverage despite lacking a coverage guarantee for covariate shift. For instance, in Figure 6 jackknife+ does lose coverage for the random forest $\widehat{\mu}$ predictor, but it does not appear to lose coverage below the target level with the neural network $\widehat{\mu}$ predictor. Figure 13 allows for a closer look at this observation, with the coverage histograms for JAW and jackknife+ on the superconductivity dataset for both random forest and neural network $\widehat{\mu}$ predictors. In Figure 13 there

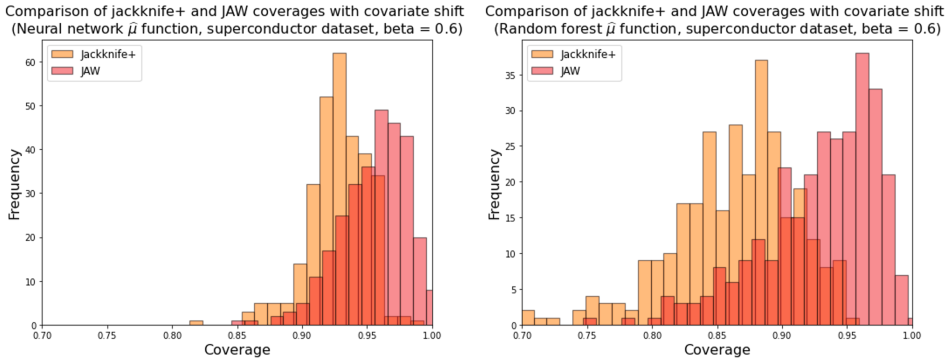

Figure 13: Comparison of the histogram of coverage on Superconductor dataset under covariate shift on the first principal component of the data, with tilting parameter $\beta = 0.6$. JAW still achieves high coverage while jackknife+ loses coverage significantly for the random forest $\widehat{\mu}$ predictor (right). For the neural network $\widehat{\mu}$ predictor (left), jackknife+ does not substantially lose coverage, while JAW has marginally higher coverage, illustrating minimal benefit of JAW over jackknife+ in this case. This is 300 replicates of the experiments.

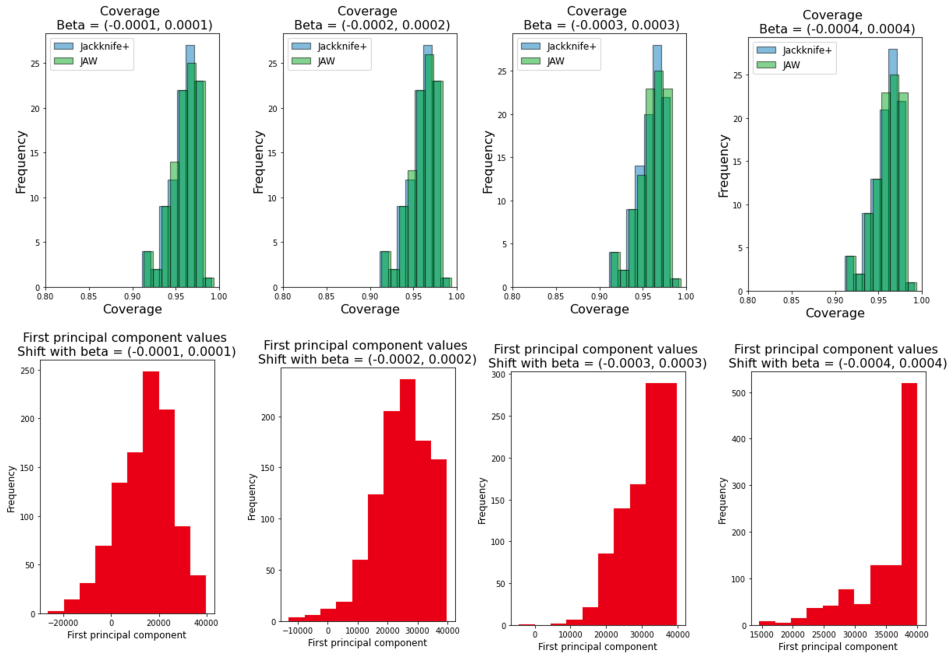

Figure 14: JAW and jackknife+ coverage for different levels of covariate shift levels on the wave energy converters dataset. Each column corresponds to a different level of shift, with increasing shift towards the right. The top row compares JAW (green) and jackknife+ (blue) coverage for a given shift level. The bottom row depicts the first principal component of the data at a given shift level. Neither jackknife+ nor JAW lose coverage at any tested shift level. This is 100 replicates of the experiments.

does appear to be a slight loss of coverage for the jackknife+ with neural network $\widehat{\mu}$ predictor, but not as significant of a loss of coverage as with a random forest $\widehat{\mu}$.

A stronger example were jackknife+ appears to not lose coverage under covariate shift is the wave dataset, where JAW and jackknife+ appear to have similar coverage (Figure 6). Figure 14 examines this observation more closely by comparing JAW and jackknife+ coverage histograms corresponding to increasing levels of covariate shift. For the wave dataset, jackknife+ does not seem to lose coverage regardless of the extent of covariate shift.

Though we leave detailed analysis of the conditions that cause jackknife+ to lose coverage or not for future work, we conjecture that jackknife+ loss of coverage may be related covariate shift that makes difficult-to-predict datapoints more likely in the test distribution, and conversely that jackknife+ may not lose coverage when covariate shift does not make difficult-to-predict datapoints more likely in the test distribution. That is, the covariate shift method we use—exponential tilting—causes rare training points to be more common in the test distribution based on the β used for tilting, but our conjecture is that the rarity of a datapoint in the training distribution does not necessarily determine how difficult that point is to predict. If rare but easy-to-predict datapoints are made more common due to exponential tilting, then this could explain why jackknife+ does not lose coverage in some cases as in Figure 14, though this conjecture requires further investigation.

C Code and computational details

C.1 Code:

https://drive.google.com/drive/folders/11T4c4ZTZFE6Up3ln5TYmMR8fxeBBRk4E?usp=sharing

C.2 Computational details

All experiments were performed on an institutional high performance computing cluster using 10 CPUs with a total of 50GB of memory.